JOC The Journal of Organic Chemistry

Article

pubs.acs.org/joc

Competitive 1,2-C Atom Shifts in the Strained Carbene Spiro[3.3]hept-1-ylidene Explained by Distinct Ring-Puckered Conformers

Murray G. Rosenberg,[‡] Theodor Schrievers,[§] and Udo H. Brinker*[,†,‡]

[†]Institute of Organic Chemistry, University of Vienna, Währinger Strasse 38, A-1090 Vienna, Austria

[‡]Department of Chemistry, The State University of New York at Binghamton, P.O. Box 6000, Binghamton, New York 13902-6000, United States

Supporting Information

ABSTRACT: Spiro[3.3]hept-1-ylidene is a markedly strained carbene reaction intermediate that was generated by high-vacuum flash pyrolysis (HVFP) of the corresponding *p*-tosylhydrazone sodium salt. Five hydrocarbons were produced from the Bamford−Stevens reactant in 82% overall yield. The carbene undergoes two [1,2]-sigmatropic rearrangements via competing 1,2-C atom shifts. Ring-contraction yields cyclopropylidenecyclobutane, while ring-expansion affords bicyclo[3.2.0]hept-1(5)-ene. The ring contraction is regiospecific despite the formation of some 1-methylenespiro[2.3]hexane. It does *not* originate from the carbene under HVFP conditions. Instead, it comes from a methylenecyclopropane-type rearrangement of chemically activated cyclopropylidenecyclobutane. Similarly, some chemically activated bicyclo[3.2.0]hept-1(5)-ene rearranges to 1,2-dimethylenecyclopentane via electrocyclic ring-opening. Accounting for the conversion of primary products to secondary ones, relative yields indicate that ring-contraction within the carbene prevails over ring-expansion by a factor of 6.7:1. Computational chemistry was used to assess the structures, conformations, energies, strain energies, transition states, and activation energies of these rearrangements with the goal of explaining product selectivities. The dual-ringed carbene is predicted to assume four distinct geometric conformations that have a bearing on transition-state selection. The reactive cyclobutylidene units of two conformers are significantly puckered, like cyclobutylidene itself, while those of the other two are flatter. The selectivity of the title carbene is compared with that of spiro[2.3]hex-4-ylidene.

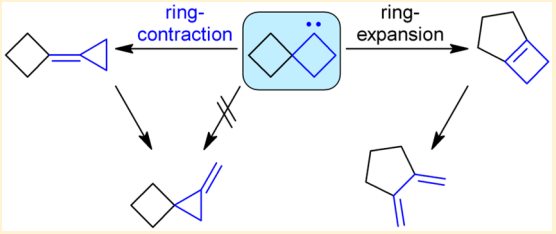

INTRODUCTION

Carbenes are neutral molecules that feature a *di*valent C atom.[1−7] Stabilizing *tetra*valency is restored when the hypovalent C atom obtains a Lewis octet. If possible, this occurs after fast isomerization(s).[8] Computational chemistry is now widely used to supplement the experimental results of these short-lived, high-energy reaction intermediates.[9] The carbene spiro[3.3]hept-1-ylidene (**1**) (Figure 1a) is a 2,2-dialkyl-substituted derivative (Figure 1b) of the small-ring carbene cyclobutylidene (**2**)[10] (Figure 1c). Spiro[2.3]hex-4-ylidene (**3**)[11−13] is one, too (Figure 1d). Carbene **1** is a homologue of **3**, which in turn could be seen as "2°-norspiro[3.3]hept-1-ylidene." The remarkable thing about carbene **3** is that, in lieu of 1,1′-bi(cyclopropylidene) (**4**), 1-methylenespiro[2.2]pentane (**5**), and spiro[2.3]hex-4-ene (**7**), it forms bicyclo[2.2.0]hex-1(4)-ene (**6**) exclusively by ring-*expansion* (Scheme 1).[11−13] This [1,2]-sigmatropic rearrangement is atypical of cyclobutylidenes[10] because 1,2-C atom shifts invariably lead to ring-*contraction* products. Thus, a study of carbene **1** was undertaken to determine the proclivity of its 1,2-C atom shift(s).

Cyclobutylidenes can be trapped *inter*molecularly by alkenes[14] and alkynes,[15] but this report delves into their *intra*molecular isomerizations.[14−17] The spin multiplicity of cyclobutylidenes,[10] due to the two nonbonding electrons, is uncharacteristic of dialkylcarbenes. The ring-enforced small bond angle of the bicoordinate C atom raises the triplet-state energy, thereby permitting a singlet ground electronic state.

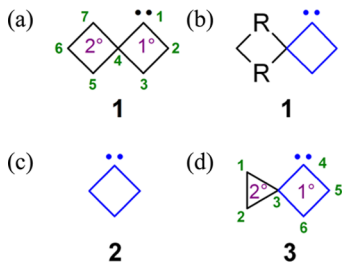

Figure 1. Strained carbene (a) spiro[3.3]hept-1-ylidene (**1**) is a (b) 2,2-dialkyl-substituted (R = $-CH_2-$) derivative of (c) cyclobutylidene (**2**). Carbene **1** is a homologue of (d) spiro[2.3]hex-4-ylidene (**3**), which avoids characteristic ring-contraction in favor of ring-expansion (Scheme 1).

Received: October 6, 2016
Published: December 2, 2016

DOI: 10.1021/acs.joc.6b02445
J. Org. Chem. 2016, 81, 12388−12400

Scheme 1. [1,2]-Sigmatropic Rearrangements of Carbene 3

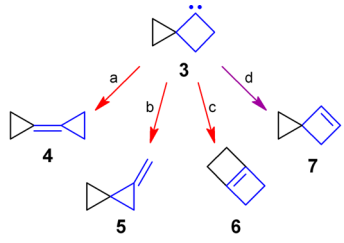

Key: (a) 1,2-C atom shift: ring-contraction (*internal*)
(b) 1,2-C atom shift: ring-contraction (*external*)
(c) 1,2-C atom shift: ring-expansion
(d) 1,2-H atom shift

The spin-paired $^1(n^2p^0)$ electron configuration of the divalent C atom also fosters classical hyperconjugation and nonclassical hypervalent C1···C3 bonding,[18−20] depending on the amount of ring-puckering.[20] The isomerization of carbene **2** to cyclobutene (**8**) (Scheme 2a) is slower than that to

Scheme 2. [1,2]-Sigmatropic Rearrangements of Cyclobutylidene (2)[a]

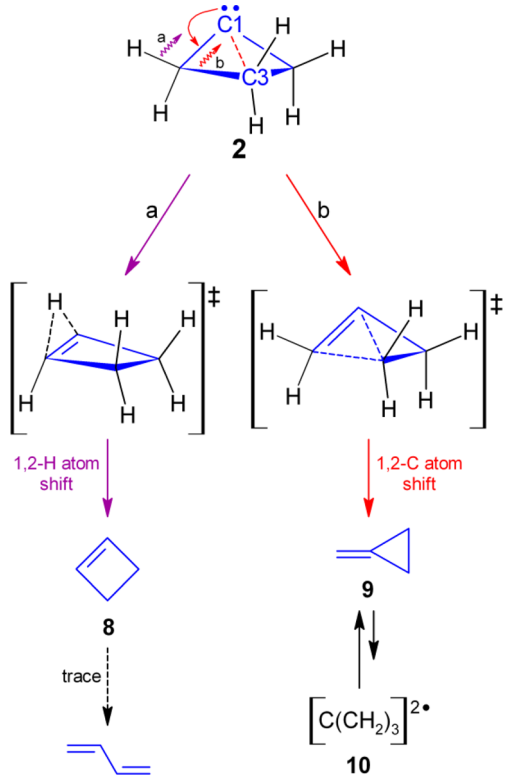

[a]Dashed red line of **2** represents its elongated nonclassical C−C single bond.

methylenecyclopropane (**9**) (Scheme 2b), which is the major product.[14−17,19,21] Energy is required to break the C1···C3 "bond"[22] in **2** (i.e., dashed red line of **2** in Scheme 2). A flatter form of **2**, which is better suited for stabilizing hyperconjugation,[20] may exist (vide infra). However, a bridging H atom introduces strain in the transition state (TS) of the 1,2-H atom shift as flattened TS(**2**/**8**) progresses to planar **8** (Scheme 2a). Whereas the formation of **8** from **2** is topologically impeded, ring-puckered **2** is conformationally predisposed to form **9** because **2** already resembles TS(**2**/**9**) (Scheme 2b). Sometimes the primary products isomerize to yield small amounts of secondary products. For example, some **8** undergoes electrocyclic ring-opening to 1,3-butadiene (Scheme 2a), and the well-known degenerate rearrangement of **9** proceeds via the trimethylenemethane (**10**) diradical (Scheme 2b).[23−26]

Gibbs free energy of activation ($\Delta G^{\ddagger}$) values for isomerizations of **2** have been computed using the CCSD(T)/DZP theoretical model:[19] (1) 1,2-H atom shift ($\Delta G^{\ddagger}$ = 9.7 kcal/mol), (2) 1,2-C atom shift ($\Delta G^{\ddagger}$ = 10.5 kcal/mol), and (3) 1,3-C−H bond insertion ($\Delta G^{\ddagger}$ = 14.6 kcal/mol). The computed $\Delta\Delta G^{\ddagger}$ between the 1,2-C atom shift **2** → **9** and the 1,2-H atom shift **2** → **8** is thus 0.8 kcal/mol.[19] From eqs 1 and 2, one arrives at a **9**:**8** ratio of 0.26 at T = 25 °C. However, this ratio is contrary to those established by numerous experiments. Ring-contraction is decisively favored (Scheme 2b) with a **9**:**8** ratio of (8.7 ± 4):1.[14−17,19,21] The experimental $\Delta\Delta G^{\ddagger}$ is thus (−1.2 ± 0.3) kcal/mol at T = 25 °C, according to eq 2. It is worth noting that the product selectivity of **2** does not reflect the amount of ring-strain energy (E_s) present in each product. The E_s value of **9** is 39.5 kcal/mol whereas that for **8** is only 28.7 kcal/mol.[27−29] These values are affirmed in this report.

$$\mathbf{9}:\mathbf{8} = e^{-\Delta\Delta G^{\ddagger}/RT} \quad (1)$$

$$\Delta\Delta G^{\ddagger} = [\Delta G^{\ddagger}_{(\mathbf{2}\rightarrow\mathbf{9})} - \Delta G^{\ddagger}_{(\mathbf{2}\rightarrow\mathbf{8})}] = -RT\ \ln(\mathbf{9}:\mathbf{8}) \quad (2)$$

2-Alkylcyclobutylidenes **11** yield alkylidenecyclopropanes and alkylcyclobutenes to a lesser extent (Scheme 3).[16,30−32]

Scheme 3. Reactions of 2-Alkylcyclobutylidenes 11

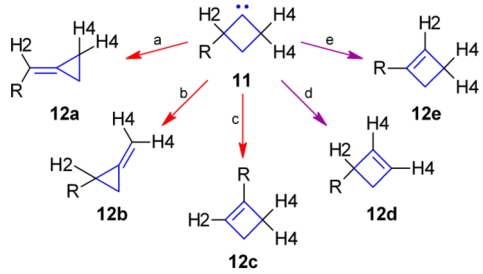

Key: (a) 1,2-C atom shift: ring-contraction (*internal*)
(b) 1,2-C atom shift: ring-contraction (*external*)
(c) 1,2-C atom shift: alkyl group (R) migration
(d) 1,2-H atom shift
(e) 1,2-H atom shift

The type of carbene precursor used (e.g., *gem*-dibromo compound[16] or *p*-tosylhydrazone alkali salt[17]) and the reaction conditions (e.g., T = −78 to 0 °C/RLi/Et_2O or T = 120 to 310 °C/p = (0.1−1.0) × 10^{-4} Torr) affect the scope of the isomerizations. For example, the debromination of 2-alkyl-1,1-dibromocyclobutanes produces alkylidenecyclopropanes **12a** in high yield (Scheme 3a), whereas alkylcyclobutenes **12c**−**e** are not formed at all (Scheme 3c−e).[30] Carbene **1** should undergo a 1,2-C atom shift leading to regiospecific 1°-ring-contraction (cf. Scheme 3a and Figure 1a, b), but it might also undergo a 2°-ring-expansion (cf. Scheme 3c and Figure 1a,b,d), as does carbene **3** (cf. Scheme 1), because it features an embedded 2,2-dialkyl-substituted cyclobutylidene (Figure 1b).

RESULTS AND DISCUSSION

Spiroannulation of cyclobutanone was achieved herein using 1-bromo-1-ethoxycyclopropane (**13**)[33−36] (Scheme 4). This

DOI: 10.1021/acs.joc.6b02445
J. Org. Chem. 2016, 81, 12388−12400

Scheme 4. Synthesis of Carbene 1 Precursor

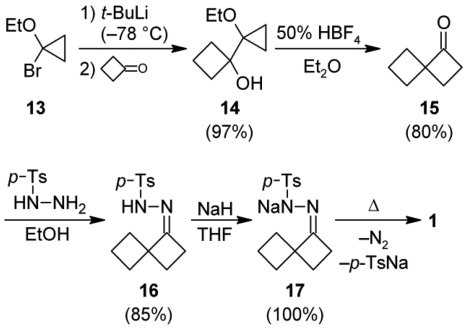

method gave spiro[3.3]heptan-1-one (**15**)[37] in 78% overall yield. The corresponding Bamford−Stevens[32,38] reactant **17** was efficiently fragmented using a high-vacuum flash pyrolysis (HVFP) apparatus (see Figure S22) to liberate carbene **1** (Scheme 4).

Five hydrocarbons were obtained in 82% overall yield upon HVFP (T = 250 °C; $p = 9 \times 10^{-4}$ Torr) of Bamford−Stevens reactant **17**. The product set profile listed in Table 1 shows

Table 1. Products from HVFP of Bamford−Stevens Reactant 17[a]

Product	Yield[b] (rel.%)
 **18**	69.3
 **19**	17.0
 **20**	8.6
 **21**	4.3
C_7H_{10} [c] **22**	0.8

[a]Reaction conditions: T = 250 °C; $p = 9 \times 10^{-4}$ Torr. [b]Overall yield = 82%. [c]See Chart 1.

their relative percentages. Standard 1-D NMR, IR, and MS experiments were performed to identify the products from known spectra. The major product was cyclopropylidenecyclobutane (**18**)[39−43] followed by 1-methylenespiro[2.3]hexane (**19**).[39,40,44] Lesser amounts of bicyclo[3.2.0]hept-1(5)-ene (**20**)[11,12,45−47] and 1,2-dimethylenecyclopentane (**21**)[45,48,49] were also formed. An unidentified hydrocarbon (**22**) was formed in trace amounts. Plausible candidates are shown in Chart 1: (1) spiro[bicyclo[1.1.0]butane-2,1′-cyclobutane] (**22a**), (2) *trans*-tricyclo[3.2.0.0^{1,4}]heptane (*trans*-**22b**),[50] (3) spiro[3.3]hept-1-ene (**22c**),[51] and (4) (prop-2-en-1-ylidene)-cyclobutane (**22d**).

Chart 1. Possible Structures of Trace Product 22

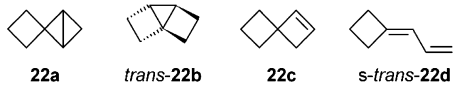

The rates of interconversion and positions of equilibria for the thermal rearrangement of **18** to **19** (Scheme 5) have been

Scheme 5. Methylenecyclopropane-Type Rearrangement of 18 to 19

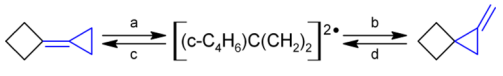

assessed at T = 190 to 220 °C and p < 100 Torr.[39,40] Higher pressures caused **18** to dimerize to tetraspiro-[2.0.2^4.0.3^7.0.3^{11}.0^3]tetradecane.[40] In the same fashion, **4** dimerizes to tetraspiro[2.0.2^4.0.2^7.0.2^{10}.0^3]dodecane.[52] When the data for **18** ⇌ **19** are extrapolated to T = 250 °C, the **18**:**19** ratio becomes 1.12:1, assuming ΔH and ΔS vary insignificantly from T = 190−250 °C. Isomers **18** and **19** should have almost equal Gibbs free energy (ΔG) values because K_{eq} is close to unity. The empirical $\Delta\Delta E = \Delta E(\mathbf{18}) - \Delta E(\mathbf{19}) = -0.39$ kcal/mol was confirmed in this report using computational chemistry (vide infra). The cyclobutylidene(dimethylene)-methane (**23**) diradical is a plausible reaction intermediate in the equilibrium **18** ⇌ **19** (Scheme 5). The activation energy (E_a) for **18** → **19** (Scheme 5a) is reported to be (39.7 ± 2) kcal/mol with a frequency factor (A) of 1.8×10^{14} s^{-1}.[39,40] When the Arrhenius activation parameters are converted into those of the unimolecular Eyring equation,[53] the data entail a $\Delta G^{\ddagger}$ value of 36.9 kcal/mol (Scheme 5a).

The HVFP of Bamford−Stevens reactant **17** resulted in an **18**:**19** ratio of 4.08:1 (Table 1), which is rapidly preserved as the isomers are physically trapped at T = −196 °C. This proportion suggests that internal ring-contraction **1** → **18** (Scheme 6a) surpasses external ring-contraction **1** → **19** (Scheme 6b) by a factor of 4.08 and that $\Delta\Delta G^{\ddagger}$ for the two ring-contractions in **1** is −1.5 kcal/mol at T = 250 °C,

Scheme 6. Potential Rearrangements of Carbene 1

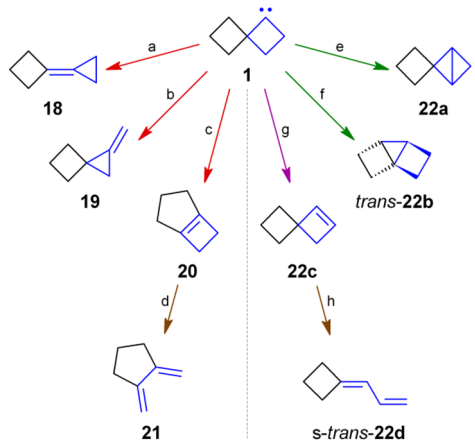

Key: (a) 1,2-C atom shift: ring-contraction (*internal*)
(b) 1,2-C atom shift: ring-contraction (*external*)
(c) 1,2-C atom shift: ring-expansion
(d) electrocyclic ring-opening
(e) 1,3-C–H bond insertion: *intra*annular
(f) 1,3-C–H bond insertion: *inter*annular
(g) 1,2-H atom shift
(h) electrocyclic ring-opening

DOI: 10.1021/acs.joc.6b02445
J. Org. Chem. 2016, 81, 12388−12400

according to eq 3. However, the ratio and corresponding $\Delta\Delta G^{\ddagger}$ value may be severely skewed because products **18** and **19** can interconvert through diradical **23** (Scheme 5).

$$\Delta\Delta G^{\ddagger} = [\Delta G^{\ddagger}_{(\mathbf{1}\rightarrow\mathbf{18})} - \Delta G^{\ddagger}_{(\mathbf{1}\rightarrow\mathbf{19})}] = -RT\ \ln(\mathbf{18}{:}\mathbf{19}) \quad (3)$$

If some **18** is depleted during the reaction then the intrinsic **18**:**19** ratio would be greater than 4.08:1 and the $\Delta\Delta G^{\ddagger}$ value (eq 3) would be more negative than −1.5 kcal/mol. Indeed, the *exo* methylene group of **19** casts doubt on its direct formation from **1**. Recall that 2-alkyl-substituted cyclobutylidenes **11** often form alkylidenecyclopropanes **12a** regiospecifically.[30] The preference for **12a** (Scheme 3a) can be traced back to its *internal* C−C double bond, which is more highly substituted than the *external* C−C double bond of **12b** (Scheme 3b). A likely resolution involves chemical activation (see Figure S37),[54,55] which is commonly observed for carbene reactions that are initiated by HVFP.[56,57] Although the $\Delta G^{\ddagger}$ value of 36.9 kcal/mol for the intramolecular rearrangement **18** → **19** (Scheme 5a) is substantial, it can be readily overcome because the energy released from **1** → **18** (cf. A → C in Figure S37) is ∼−60 kcal/mol. An accelerated isomerization of **18** to **19** (cf. C → E in Figure S37) is plausible because the excess energy of vibrationally excited **18*** cannot be dissipated well. Collisional deactivation by the other gas-phase molecules in the HVFP chamber is infrequent. To support the hypothesis that **19** does not stem from **1**, E_a values for **1** → **18** and **1** → **19** were computed and compared to obtain a theoretical ratio of **18**:**19** (vide infra). The Boltzmann distribution treatment of **1** in eq 3 does not provide absolute $\Delta G^{\ddagger}$ values for these elementary steps. As noted, the computed $\Delta G^{\ddagger}$ value for 1,2-C atom shift in cyclobutylidene was reported to be 10.5 kcal/mol.[19] However, a more rigorous value of 6.7 kcal/mol was recently reported.[58] This value accords better with the experimental **9**:**8** ratio and it should serve as a benchmark concerning the ring-contraction of **2** and its derivatives, such as **1**.

Like **18**, product **20** is chemically activated when it is formed by HVFP (Scheme 6c). That is because some **21** was formed from **20** (Scheme 6d). Although E_s is relieved by **20** → **21**, the E_a barrier for the electrocyclic ring-opening of the four-membered ring must be overcome. Since the first step **1** → **20** is very exothermic (cf. A → C in Figure S37),[55−57] vibrationally excited **20*** has ample excess energy for the secondary step (cf. C → E in Figure S37) to occur. When the secondary byproducts are included, the tendency for the ring-contraction(s) vs ring-expansion of **1** can be quantified by calculating the relative percentages of (**18** + **19**) vs (**20** + **21**), as listed in Table 1. An empirical ratio of 6.7:1 is obtained, but this value could be too high. If conjugated diene **21** oligomerized during HVFP or workup then a lower percentage of **21** would have been integrated in the gas chromatography (GC) analysis. This may explain why only 82% of the theoretical yield from **17** was obtained (Table 1). In any case, this ratio is conversely related to the unusual (**4** + **5**):**6** ratio of 0:1 observed for **3** (Scheme 1),[11−13] wherein ring-expansion occurs exclusively.

Rearrangements of carbene **1** by means other than 1,2-C atom shifts were explored. Four candidates were proposed for the identity of **22** (Chart 1). The formation of each involves well-known carbene chemistry.[1−8] Spiro[bicyclo[1.1.0]butane-2,1′-cyclobutane] (**22a**) would be formed by an *intra*annular 1,3-C−H bond insertion reaction of **1** (Scheme 6e). This may be possible if the 1°-ring in **1** is significantly puckered, as is the case with cyclobutylidene (**2**). Even so, **2** itself does not undergo a 1,3-C−H bond insertion to bicyclo[1.1.0]butane. The substantial amount of ring-strain energy in **22a** makes it an unlikely contender for the identity of **22**. *trans*-Tricyclo-[3.2.0.0^{1,4}]heptane (*trans*-**22b**)[50] would be formed by an *inter*annular 1,3-C−H bond insertion reaction of **1** (Scheme 6f). Buckled "house"ane derivative *trans*-**22b** features a central cyclopropane and two antiperiplanar four-membered rings. The formation of a "house"ane from a 2,2-dialkyl-substituted cyclobutylidene, by a related 1,3-C−H bond insertion reaction, is already known.[59] Alkylcarbenes often undergo rapid 1,2-H shifts to form alkenes. However, this rearrangement is much less pronounced in 2-alkylcyclobutylidenes (e.g., Scheme 3d, e).[30−32] Spiro[3.3]hept-1-ene (**22c**)[51] would arise from a 1,2-H shift in **1** (Scheme 6g). Although there is acute bending of the nominally sp^2-hybridized C1 and C2 atoms in **22c**, angle strain within such a C−C double bond is only a minor barrier toward its formation.[12,28,60] If **1** yields vibrationally excited **22c***, then chemical activation would facilitate electrocyclic ring-opening to conjugated diene **22d** (Scheme 6h; cf. C → E in Figure S37). Thus, candidates **22c** (Scheme 7) and **22d** (Scheme 8) were independently synthesized, but still no conclusion could be made about the identity of trace hydrocarbon **22**.

Scheme 7. Independent Synthesis of Spiro[3.3]hept-1-ene (22c)

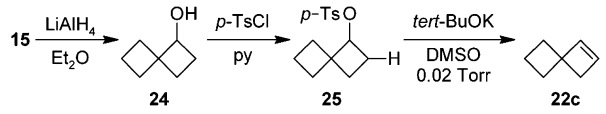

Scheme 8. Independent Synthesis of (Prop-2-en-1-ylidene)cyclobutane (22d)

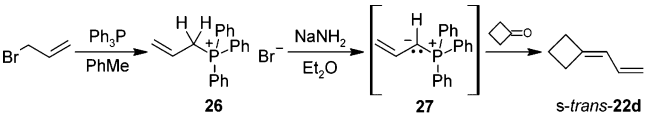

Computational chemistry was used to model cyclobutylidenes **1**−**3**. The four-membered ring of cyclobutane is not flat for various reasons (e.g., the eight C−H bonds would all be eclipsed). Torsional strain is relieved by ring-puckering. Cyclobutane's ring-puckering dihedral angle (ϕ) is 35° and the ring-puckering inversion barrier TS, through flat cyclobutane, is 1.5 kcal/mol.[61,62] Torsional strain in spiro[3.3]-heptane[63] is reduced by ring-puckering in both four-membered rings.[62,64] Carbene **1** is a similar molecule. Of course, its four-membered rings are different from each other (Figure 1a). Nevertheless, *both* four-membered rings of **1** pucker to reduce strain. Its dual four-membered rings are stabilized by ring-puckering of the 1°- and 2°-rings (Figure 1a). 2°-Ring-puckering inversion in **1** (Figure 1a) yields two geometric isomers (+*ac*)-**1** (Figure 2a) and (−*ac*)-**1** (Figure 2b). 1°-Ring-puckering inversion in **1** (Figure 1a) interconverts optical isomers **1** (i.e., {(±*ac*)-}**1** in Figure 2c) and *ent*-**1** (i.e., *ent*-{(±*ac*)-}**1** in Figure 2d). Besides inversion, two discrete amounts of 1°-ring-puckering in **1** lead to geometric conformers **1a** and **1b** (vide infra). Four geometric conformers are therefore possible because 2°-ring-puckering also occurs: (1) (+*ac*)-**1a**, (2) (−*ac*)-**1a**, (3) (+*ac*)-**1b**, and (4) (−*ac*)-**1b**. If the optical isomers of **1** (i.e., *ent*-**1**) are included then there are a total of 2 × 2^2 = 8 conformers. Equilibrium geometries of **1** were obtained using the (U)B3LYP/6-31G(d) theoretical

DOI: 10.1021/acs.joc.6b02445
J. Org. Chem. 2016, 81, 12388−12400

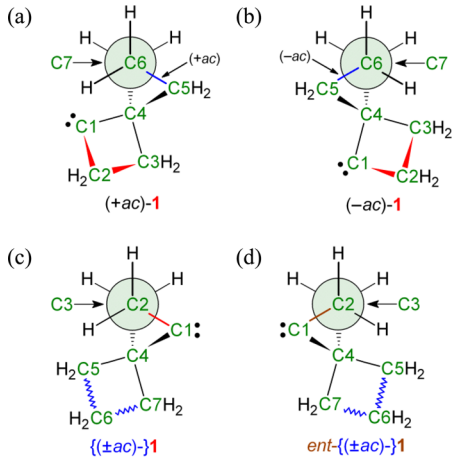

Figure 2. 2°-Ring-puckering inversion in carbene **1** gives (a) positive anticlinal and (b) negative anticlinal geometric conformers (+*ac*)-**1** and (−*ac*)-**1**, respectively. 1°-ring-puckering inversion in **1** results in the (c) {(±*ac*)-}**1** and (d) *ent*-{(±*ac*)-}**1** optical conformers.

model. The 3-D Cartesian coordinates and corresponding 2-D renderings (Figure S34) are available in the Supporting Information.

In this report, a cyclobutylidene ϕ_n value represents the acute deviation of the three-point C2−C1−C4 α-plane from the three-point C2−C3−C4 β-plane reference (Figure 3).

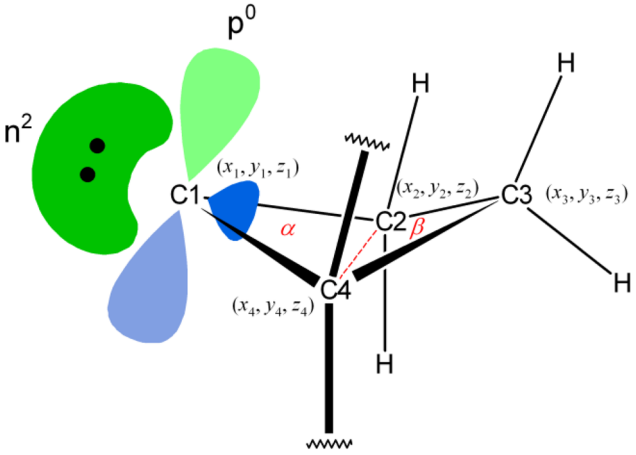

Figure 3. Ring-puckering dihedral angle (ϕ_n) values of cyclobutylidenes were based on the asymmetric model shown above (see Figure S35 in the Supporting Information for more details).

Mathematical details are presented in the Supporting Information (cf. Figure S35). Values of ϕ_n were calculated by measuring those of dihedral angle ω_n(C1−C2−C4−C3), using a graphical user interface[65] and then by applying the $\omega \rightarrow \phi$ relation plotted in Figure S36 (see Supporting Information). Geometric conformers **1a** and **1b** are easily distinguished by their markedly different 1°-ring-puckering dihedral angle ($\phi_{1°}$) values (Figure 4). The curves in Figure 4 were obtained by varying $\phi_{1°}$ while leaving the 2°-ring unconstrained. The $\phi_{1°}$ values of (±*ac*)-**1a** are ∼45° more than those of (±*ac*)-**1b**, which are slightly affected by 2°-ring puckering. The 2°-ring-puckering dihedral angle ($\phi_{2°}$) values of **1a** and **1b** (Figure 5), with unconstrained 1°-rings, were found using dihedral angle $\omega_{2°}$(C4−C7−C5−C6) and Figure S36 (see the Supporting Information). The algebraic sign of $\phi_{2°}$ thus matches the

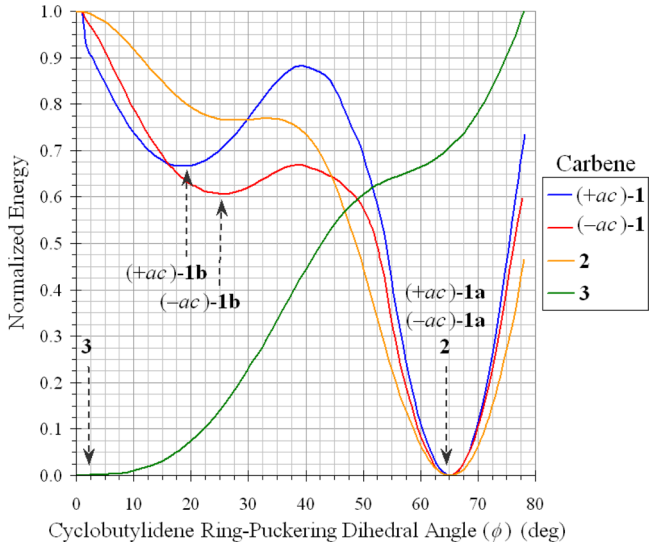

Figure 4. Energies of cyclobutylidenes **1** and **2** are minimized by pronounced ring-puckering (ϕ = 65°), which shields the divalent C atom. The presence of the conjoined 2°-ring in **1** (Figure 1a) leads to four geometric conformers (i.e., four minima): (a) (+*ac*)-**1a**, (b) (+*ac*)-**1b**, (c) (−*ac*)-**1a**, and (d) (−*ac*)-**1b**. Cyclobutylidene **3** (Figure 1d) is completely different because its geometry is optimal when the 1°-ring is *flat*. The energy profiles were computed using the B3LYP/6-31G(d)//B3LYP/6-31G(d) theoretical model and normalized according to eq 4.

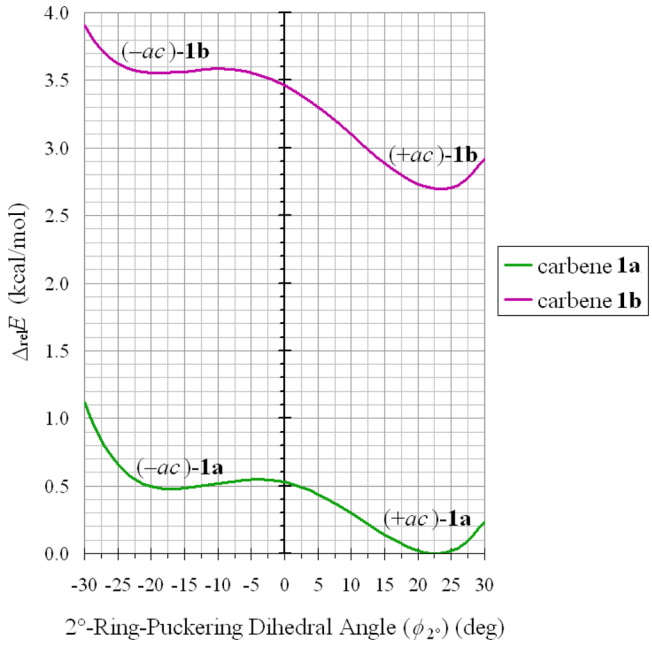

Figure 5. 2°-Ring-puckering in **1a** leads to geometric isomers (+*ac*)-**1a** and (−*ac*)-**1a**, whereas the less-ring-puckered form **1b** gives (+*ac*)-**1b** and (−*ac*)-**1b**. The energy profiles were computed using the B3LYP/6-31G(d)//B3LYP/6-31G(d) theoretical model.

corresponding (+*ac*) or (−*ac*) stereodescriptor of **1**. Similarly, the ϕ values of **2** (Figure 1c) were found using ω(C1−C2−C4−C3) and Figure S36 (see the Supporting Information), while the $\phi_{1°}$ values of **3** (Figure 1d) were found using $\omega_{1°}$(C4−C5−C3−C6) and Figure S36 (see the Supporting Information).

DOI: 10.1021/acs.joc.6b02445
J. Org. Chem. 2016, 81, 12388−12400

Table 2. Computed Measurements of Carbene 1[a]

carbene	$\Delta_{rel}E$ (kcal/mol)	$\phi_{1°}$[b] (deg)	$\phi_{2°}$[b] (deg)	θ(C4−C1−C2) (deg)	r(C1−C3) (Å)
^{1}(+*ac*)-**1a**	[0][c]	65	22	102	1.75[d]
^{1}(−*ac*)-**1a**	0.6	65	−17	102	1.75[d]
^{1}(+*ac*)-**1b**	1.1	19	23	87	2.22
^{1}(−*ac*)-**1b**	2.4	25	−18	87	2.20
^{3}(+*ac*)-**1**	5.2	0	25	99	2.06
^{3}(−*ac*)-**1**	5.1	0	−24	99	2.06

[a]Computed using the UQCISD(T)(fc)/6-311G(d,p)//(U)B3LYP/6-31G(d) theoretical model. See the Computational Methods and the Supporting Information for details. [b]See the Supporting Information (Figure S35) and related text for details. [c]Defined as a reference state. [d]See ref 22.

The energy profiles of Figure 5 were computed by varying the $\phi_{2°}$ values of **1a** and **1b** while leaving each 1°-ring unconstrained. Three trends are conspicuous: (1) the energy of geometric conformer **1a** is always lower than that of **1b**, (2) the energy difference (ΔE) between them varies little as a function of $\phi_{2°}$, and (3) 2°-ring-puckering inversion through $\phi_{2°} = 0°$ does not affect the energies of **1a** and **1b** much. However, the conformation of the 2°-ring can influence which conformation the reactive 1°-ring of **1** must adopt for each TS.

The energy profiles of carbenes **1**−**3** shown in Figure 4 were computed by varying $\phi_{(1°)}$ of the four-membered rings. Each curve is normalized according to eq 4 in order to compare it with the others. The original plots with vertical axes of E(hartree) are available in the Supporting Information (cf. Figures S28−S33). The curves for (+*ac*)-**1** and (−*ac*)-**1** show that (+*ac*)-**1a** ($\phi_{1°} = 65°$) and (−*ac*)-**1a** ($\phi_{1°} = 65°$) are lower in energy than the less-ring-puckered conformers (+*ac*)-**1b** ($\phi_{1°} = 19°$) and (−*ac*)-**1b** ($\phi_{1°} = 25°$), respectively. Furthermore, the steep gradients found for carbenes **1a** suggest that they are more persistent than carbenes **1b**. The energy profiles for the *ent*-**1** isomers (Figure 2d) are mirror images of those for the **1** isomers, with respect to the 1°-ring-puckering inversion energy barriers at $\phi_{1°} = 0°$, so they are omitted in Figure 4.

$$\text{normalized energy} = \frac{E - E_{min}}{E_{max} - E_{min}} \quad (4)$$

Monocyclic **2** was computed to have a markedly ring-puckered conformation ("**2a**"; $\phi = 65°$) based on the ring-puckering dihedral angle ω(C1−C2−C4−C3) (cf. Figure 3). This result affirms a previous report.[20] A flatter conformer of **2** ("**2b**"; $\phi = 28°$) is unsteadily positioned on a shoulder-like region of the potential energy profile (Figure 4). Its authenticity depends on the theoretical model used.[20] The curve for carbene **3** is strikingly different from those of **1** and **2** (Figure 4). Its 1°-ring-puckering inversion point at $\phi_{1°} = 0°$, for which the four-membered ring is flat, does not represent a *transition state* energy barrier between conformers. It signifies the *equilibrium geometry* of **3** (Figure 1d, Figure 6).

There is a cyclopropylcarbene-like unit in **3** comprising the C1−C4 atoms (Figure 6). It exemplifies the bisected form of cyclopropylcarbene,[66] wherein the plane of the n orbital bisects the three-membered ring. The four-membered ring, of course, prevents rotation of the C3−C4 bond but it also ensures that the bisected form remains in the *exo* form,[67] with regard to the parent cyclopropylcarbene. The fragmentation of **3** to ethene and cyclobutyne[68] is thereby precluded. The crucial aspect is the interaction of the highest filled Walsh orbital of the three-membered ring and the empty p orbital on the divalent C atom (Figure 6). The Walsh-to-p orbital interaction is maximized

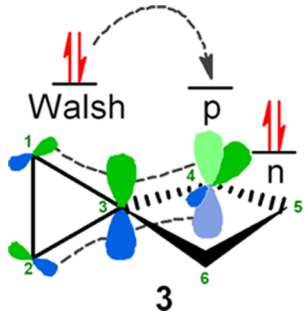

Figure 6. Atypical regiospecificity of **3** (Scheme 1) is due to its *planar* four-membered ring, which maximizes interaction between the highest filled Walsh orbital of the three-membered ring and the unfilled p orbital of the divalent C atom. The necessary orbital alignment is impaired with increased 1°-ring-puckering, and the energy of **3** rises concomitantly (Figure 4).

when the pertinent orbitals are aligned. For this, planarity of the four-membered ring is key. The contiguous orbital interaction is responsible for the regiospecific ring-expansion of **3** to **6** (Scheme 1c). Ring-expansion of the carbene spiro[2.4]hept-4-ylidene (**28**)[45] supports the validity of this hypothesis (Figure 7). Only compound **20** was formed from **28** when it was

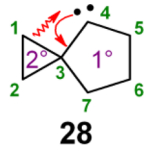

Figure 7. Carbene spiro[2.4]hept-4-ylidene (**28**) undergoes exclusive ring-expansion to **20**. This atypical regiospecificity is akin to **3** → **6** (Scheme 1c).

generated by HVFP.[11,12] Carbene **28** must have a significant Walsh-to-p orbital interaction (cf. Figure 6). The five-membered 1°-ring of **28** is expected to be almost flat. The four-membered 1°-rings of (±*ac*)-**1b** are somewhat puckered (Figure 4), but the 2°-ring of **1b** has no Walsh orbitals because it is a four-membered ring. Hence, the **1** → **20** ring-expansion reaction is not enhanced (Scheme 6c), as is the case for the **3** → **6** and **28** → **20** ring-expansion reactions.

Relative energies and select measurements of the optimized geometric conformers of singlet spiro[3.3]hept-1-ylidene (^{1}**1**) and triplet spiro[3.3]hept-1-ylidene (^{3}**1**) are listed in Table 2. There are four distinct geometric conformers of ^{1}**1** (i.e., ^{1}(+*ac*)-**1a**, ^{1}(−*ac*)-**1a**, ^{1}(+*ac*)-**1b**, and ^{1}(−*ac*)-**1b**), but there are only two geometric conformers of ^{3}**1** (i.e., ^{3}(+*ac*)-**1** and ^{3}(−*ac*)-**1**). Although the 2°-ring of ^{3}**1** experiences ring-puckering, the 1°-

DOI: 10.1021/acs.joc.6b02445
J. Org. Chem. 2016, 81, 12388−12400

Table 3. Computed Measurements of Carbene 1 Transition States and Products[a]

molecule	$\Delta_{rel}E$[b] (kcal/mol)	$\phi_{1°}$[c] (deg)	$\phi_{2°}$[c] (deg)	θ(C4−C1−C2)[d] (deg)	r(C1−C3) (Å)
TS((+*ac*)-**1a**/**18**)	4.0	81	23	110	1.64
TS((−*ac*)-**1a**/**18**)	3.9	80	−18	110	1.65
18	−51.1	±180	±14	212	1.47
TS((+*ac*)-**1a**/(+*ac*)-**19**)	11.3	70	15	115	1.78
(+*ac*)-**19**	−50.7	±180	19	211	1.48
TS((−*ac*)-**1a**/(−*ac*)-**19**)	9.1	84	−18	113	1.61
(−*ac*)-**19**	−50.7	±180	−20	211	1.48
TS((+*ac*)-**1b**/**20**)	3.8	−10	23	86	2.23
20	−71.0	0	±15	95	2.11
TS((+*ac*)-**1a**/**22a**)	15.1	73	18	89	1.74
TS((−*ac*)-**1a**/**22**)	15.3	73	−16	89	1.74
22a	−43.8	78	±19	99	1.51
TS((+*ac*)-**1b**/*trans*-**22b**)	6.9	−19	8	86	2.23
trans-**22b**	−52.2	−8	8	88	2.21
TS((+*ac*)-**1b**/(+*ac*)-**22c**)	8.1	−3	28	87	2.23
(+*ac*)-**22c**	−60.1	0	26	94	2.10
TS((−*ac*)-**1b**/(−*ac*)-**22c**)	9.4	−4	−24	87	2.23
(−*ac*)-**22c**	−60.3	0	−26	95	2.10

[a]Computed using the UQCISD(T)(fc)/6-311G(d,p)//B3LYP/6-31G(d) theoretical model. See the Computational Methods and the Supporting Information for details. [b]Relative to (+*ac*)-**1a**. [c]See the Supporting Information (Figure S35) and related text for details. [d]Atom numbering preserved from **1** (Figure 1a).

ring of ^{3}**1** has only one conformation. It is flat (i.e., $\phi_{1°} = 0°$). Thus, the 1°-ring-puckering inversion point at $\phi_{1°} = 0°$ (Figure 4) marks the *equilibrium geometry* of ^{3}**1** and of ^{1}**3**. Evidently, there is no energetic benefit (and possibly a detriment) from any cyclobutylidene ring-puckering if the nominally empty p orbital of the divalent C atom gains electron density from exocyclic bonding electrons or from nonbonding electrons. This appears to be the case with ^{1}**3**, due to the Walsh MO of its aptly positioned cyclopropane, and with ^{3}**1** and ^{3}**2**, which have ^{3}(n^{1}p^1) electron configurations. Furthermore, the bond angle θ(C4−C1−C2) of ^{3}**1** is 99°, which is very far from the ideal H−C−H bond angle of 133.9° in ^{3}CH$_2$.[9,69,70] Thus, it is understandable why cyclobutylidene **1** has a singlet ground state (Table 3). According to the UQCISD(T)(fc)/6-311G(d,p)//(U)B3LYP/6-31G(d) theoretical model used herein, the singlet−triplet energy gap (ΔE_{S-T}) of **3** is −9.0 kcal/mol and that of (+*ac*)-**1** is −5.2 kcal/mol. For reference, values for **2** have been reported to be −5.9 kcal/mol[20] and −9.3 kcal/mol.[58]

Figure S38 (see the Supporting Information) is provided as a general energy profile for the elementary steps presented in Table 4, which lists pertinent energy and structural data regarding the conformations of **1** and its transformations to products **18**−**22**. For example, the 1°-ring-puckering inversion E_a barrier for (+*ac*)-**1b** is 1.3 kcal/mol and that for (−*ac*)-**1b** is 2.3 kcal/mol (Table 4). Further inspection reveals that the dimensions of **1a** are more compatible with those of certain transition states, whereas **1b** more closely resembles others. However, structural similarity is no guarantee that the TS will be energetically accessible. Indeed, the isomerization reactions (Scheme 6) that confer a stabilizing Lewis octet around the divalent C atom of **1** may be selectively driven by the optimum relief of strain in either or both four-membered rings of **1**, which are conjoined by the spirocyclic C4 atom (Figure 1a). The UQCISD(T)(fc)/6-311G(d,p)//B3LYP/6-31G(d) theoretical model was used to compute relative energies and strain energies of **1** and its products to explore this idea (see Figures S23−S25 and Table 4). Details about how energy (E) values were corrected and converted to enthalpy (H) values are

Table 4. Reaction Energies Relative to Carbene (+*ac*)-1a[a−c]

A → B	A	TS(A/B)	E_a	B	ΔE
(+*ac*)-**1a** → (+*ac*)-**1b**	[0]	1.5	1.5	1.1	1.1
(−*ac*)-**1a** → (−*ac*)-**1b**	0.6	2.1	1.5	2.4	1.9
(+*ac*)-**1b** → *ent*-(+*ac*)-**1b**	1.1	2.4	1.3	1.1	0
(−*ac*)-**1b** → *ent*-(−*ac*)-**1b**	2.4	4.7	2.3	2.4	0
(+*ac*)-**1a** → (−*ac*)-**1a**	[0]	1.0	1.0	0.6	0.6
(+*ac*)-**1b** → (−*ac*)-**1b**	1.1	2.8	1.7	2.4	1.4
(+*ac*)-**1a** → **18**	[0]	4.0	4.0	−51.1	−51.1
(−*ac*)-**1a** → **18**	0.6	3.9	3.3	−51.1	−51.7
(+*ac*)-**1a** → (+*ac*)-**19**	[0]	11.3	11.3	−50.7	−50.7
(−*ac*)-**1a** → (−*ac*)-**19**	0.6	9.1	8.6	−50.7	−51.3
(+*ac*)-**1b** → **20**	1.1	3.8	2.7	−71.0	−72.0
20 → **21**	−71.0	−38.4	32.6	−90.3	−19.4
(+*ac*)-**1a** → **22a**	[0]	15.1	15.1	−43.8	−43.8
(−*ac*)-**1a** → **22a**	0.6	15.3	14.6	−43.8	−44.3
ent-(+*ac*)-**1b** → *trans*-**22b**	1.1	6.9	5.8	−52.2	−53.3
(+*ac*)-**1b** → (+*ac*)-**22c**	1.1	8.1	7.0	−60.1	−61.1
(−*ac*)-**1b** → (−*ac*)-**22c**	2.4	9.4	5.7	−60.3	−62.7
(+*ac*)-**22c** → *s-cis*-**22d**	−60.1	−25.3	34.8	−67.9	−7.9
s-cis-**22d** → *s-trans*-**22d**	−67.9	−65.5	2.4	−70.3	−2.4

[a]Computed using the UQCISD(T)(fc)/6-311G(d,p)//B3LYP/6-31G(d) theoretical model. See the Computational Methods and the Supporting Information for details. [b]Energy units are kcal/mol. [c]See the Supporting Information (Figure S38) for heading definitions.

described in the Computational Methods and the Supporting Information. The energies of C_7H_{10} molecules are reported relative to (+*ac*)-**1a** (see Figures S23−S25) because it is the lowest energy conformation of **1**. Similarly, the energies of C_4H_6 molecules are reported relative to "**2a**" (see Figure S26), and those of C_6H_8 molecules are reported relative to **3** (see Figure S27). The group equivalent method[71] was used to construct homodesmotic bond-separation reactions,[72−75] which were used to compute E_s values of **1** and related molecules (see Figures S23−S25), **2** and related molecules (see Figure S26), and **3** and related molecules (see Figure S27). The balanced chemical equations and heat of reaction ($\Delta H°$) values (T =

DOI: 10.1021/acs.joc.6b02445
J. Org. Chem. 2016, 81, 12388−12400

298.15 K; p = 1 atm) are tabulated in Table S2. Note that $E_s = -\Delta H°$ and that geometric features (e.g., *cis* vs *trans* C−C double bond) of the cyclic molecules were matched in the acyclic ones.

A rationale for the prevalence of **1** → **18** over **1** → **19** is illustrated by resonance forms of **1** (Scheme 9). Resonance

Scheme 9. Competitive 1,2-C Atom Shifts within Carbene 1

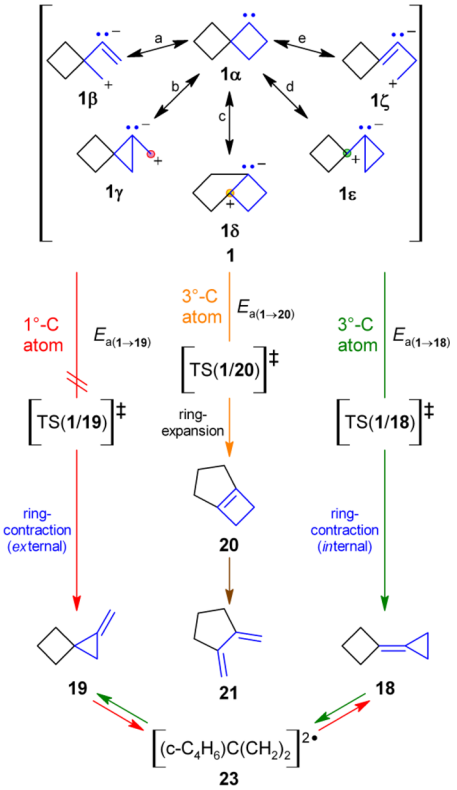

form **1α** is central because it does not exhibit destabilizing separation of unlike electric charges, as do **1β**−**1ζ**. Homoallylic forms **1β** and **1ζ** are 1,3-zwitterions that do not contribute much to the overall Lewis structure of **1**. Forms **1γ** and **1ε** are derivatives of the nonclassical bicyclobutonium ion.[76,77] Although they are 1,2-zwitterions, ylidic forms **1γ** and **1ε** are reasonable because the buildup of opposing charges can be immediately reconciled by C−C double-bond formation to **19** and **18**, respectively. Thus, **1** → **18** should prevail over **1** → **19**. The internal ring-contraction TS(**1**/**18**) resembles form **1ε** (Scheme 9d), which has positive charge on a "3°-C atom" of a "cyclopropylmethyl cation," but the external ring-contraction TS(**1**/**19**) resembles form **1γ** (Scheme 9b), which has a positive charge on a "1°-C atom" of a "cyclopropylmethyl cation." Given these factors, one must conclude that the energy of TS(**1**/**18**) is lower than that of TS(**1**/**19**). Indeed, TS((+*ac*)-**1a**/**18**) lies 7.3 kcal/mol lower than TS((+*ac*)-**1a**/(+*ac*)-**19**) and TS((−*ac*)-**1a**/**18**) lies 5.2 kcal/mol lower than TS((−*ac*)-**1a**/(−*ac*)-**19**) (Table 4). Analysis of the Boltzmann factors derived from these TS $\Delta\Delta E$ values shows that **18** is formed in 100 rel % yield and (±*ac*)-**19** is formed in 0 rel % yield. Of the two ring-contractions possible within **1**, cleavage of the more substituted C3−C4 bond dwarfs that of the C3−C2 bond (Figure 1a). The removal of spiroannulation within **1** might be the driving force behind the 1,2-C atom shift in **1** → **18**. This is not accomplished by **1** → **19**. Carbene **1** also rearranges by a rare kind of 1,2-C atom shift to form ring-expansion product **20** (Scheme 6c). This isomerization is akin to **3** → **6** (Scheme 1); however, ring-expansion **1**→**20** is dominated by ring-contraction **1**→**18** (Table 1 and Scheme 9). Resonance structures of **1** are less instructive in this case (Scheme 9).

It is clear that **20** has less E and E_s than **18** (see Figure S24), but more **18** was formed than was **20** (Table 1). A comparison of their transition-state energies from **1** must be made. A 17 rel % excess of **20** + **21** should be formed over **18** + **19** because the energy of TS((+*ac*)-**1b**/**20**) is 0.2 kcal/mol lower than that of TS((+*ac*)-**1a**/**18**) (Table 4). This is contrary to what was observed (Table 1). One possible solution is that the yield of **21** is underrepresented in Table 1 due to its oligomerization. There is another possible explanation. Although the E_a values for TS(**1**/**18**) and TS(**1**/**20**) are similar, the populations of **1a** and **1b** are not. The relative yields of **18** and **20** reflect the mechanistic rate constants for **1a** → **18** and **1b** → **20** as well as the equilibrium constant for **1a**⇌**1b**.

Tables 5 and 6 list pertinent data for the [1,2]-sigmatropic rearrangements of carbene **3**. The formation of **6** (Scheme 1) is

Table 6. Reaction Energies Relative to Carbene 3[a−c]

A → B	A	TS(A/B)	E_a	B	ΔE
3→**4**	[0]	17.5	17.5	−39.1	−39.1
3→**5**	[0]	20.5	20.5	−43.1	−43.1
3→**6**	[0]	5.6	5.6	−28.5	−28.5
3→**7**	[0]	11.0	11.0	−56.1	−56.1

[a]Computed using the UQCISD(T)(fc)/6-311G(d,p)//B3LYP/6-31G(d) theoretical model. See the Computational Methods and Supporting Information for details. [b]Energy units are kcal/mol. [c]See the Supporting Information (Figure S38) for heading definitions.

Table 5. Computed Measurements of Carbene 3 Transition States and Products[a]

molecule	$\Delta_{rel}E$[b] (kcal/mol)	$\phi_{1°}$[c] (deg)	ω(C4−C3−C2−C1)[d] (deg)	θ(C3−C4−C5)[d] (deg)	r(C4−C6) (Å)
TS(**3**/**4**)	17.5	83	−160	110	1.64
4	−39.1	±180	0	58	1.47
TS(**3**/**5**)	20.5	68	−120	113	1.82
5	−43.1	±180	−132	210	1.49
TS(**3**/**6**)	5.6	−3	−42	86	2.24
6	−28.5	0	0	95	2.11
TS(**3**/**7**)	11.0	−4	−117	86	2.23
7	−56.1	0	−118	94	2.11

[a]Computed using the UQCISD(T)(fc)/6-311G(d,p)//B3LYP/6-31G(d) theoretical model. See the Computational Methods and Supporting Information for details. [b]Relative to **3**. [c]See the Supporting Information (Figure S35) and related text for details. [d]Atom numbering preserved from **3** (Figure 1d).

DOI: 10.1021/acs.joc.6b02445
J. Org. Chem. 2016, 81, 12388−12400

the most rapid isomerization because its E_a value of 5.6 kcal/mol is the lowest (Table 6). The ring-expansion **3**→**6** occurs exclusively even though **6** has both the highest relative energy and highest ring-strain energy among the **4**−**7** product set (see Figure S27).

CONCLUSIONS

Five hydrocarbons were formed in 82% overall yield from the high-vacuum flash pyrolysis (HVFP) of Bamford−Stevens reactant **17**. Four of them were characterized as C_7H_{10} isomers: (1) cyclopropylidenecyclobutane (**18**) (69.3 rel %), (2) 1-methylenespiro[2.3]hexane (**19**) (17.0 rel %), (3) bicyclo[3.2.0]hept-1(5)-ene (**20**) (8.6 rel %), and (4) 1,2-dimethylenecyclopentane (**21**) (4.3 rel %). The fifth product was an unidentified hydrocarbon (**22**) made in trace amounts. The highly strained carbene spiro[3.3]hept-1-ylidene (**1**) was posited as a reaction intermediate mainly for two reasons: (1) the HVFP of a Bamford−Stevens reactant generally liberates the corresponding carbene and (2) products **18**−**20** can result from the isomerization of **1**. Product **21** stems from **20**. Computational chemistry was used to assess the structures, conformations, energies, strain energies, transition states, and E_a values for these rearrangements with the goal of explaining product selectivities.

Products **18**−**20** can derive from three different 1,2-C atom shifts within **1**. The viability of each [1,2]-sigmatropic rearrangement was investigated using computational chemistry. The E_a value for the direct isomerization **1** → **19** was predicted to be significantly higher than those for **1** → **18** and **1** → **20**. The carbene route to **19** could therefore be dimissed. Its presence is ancillary. Carbene **1** undergoes two competitive 1,2-C atom shifts involving ring-*contraction* to **18** and ring-*expansion* to **20**. Products **18** and **20** are formed in a chemically activated state (i.e., **18*** and **20***), because **1** is high in energy. Such is common for the HVFP method of carbene generation. The accelerated formation of secondary products **19** and **21** from **18*** and **20***, respectively, is possible because collisional deactivation of **18*** and **20*** in the gas phase is less frequent than in the condensed phase (e.g., in liquid solution). The majority of **18*** and **20*** eventually relaxes to **18** and **20**, respectively. A nondegenerate methylenecyclopropane rearrangement of **18***, which is facilitated by diradical **23**, yields **19** while **21** is formed by the electrocyclic ring-opening of **20***. The divergent 1,2-C atom shifts within **1** can be quantified by comparing the sum of **18** and **19** (i.e., ring-contraction) with that of **20** and **21** (i.e., ring-expansion). This furnishes a regioselectivity ratio of 6.7:1.

Products **18** and **19** are nearly isoenergetic: ΔE(**18**) − ΔE(**19**) = −0.39 kcal/mol. Thus, it is not surprising that extrapolation of reported **18**:**19** thermal equilibrium ratios to T = 250 °C gives an almost equimolar ratio of 1.12:1. The unequal **18**:**19** ratio of 4.08:1 observed herein is due to kinetics. The larger fraction of **18** implies that TS(**1**/**18**) is lower in energy than is TS(**1**/**19**). An analysis of the Boltzmann factors for the TS $\Delta\Delta E$ values of 7.3 kcal/mol for the + *ac* conformers and 5.2 kcal/mol for the − *ac* conformers shows that **1** is not a significant source of **19**. Between them, **18** is formed in 100 rel % yield and (±*ac*)-**19** is formed in 0 rel % yield. Hence, the 4.08:1 ratio of **18**:**19** obtained from **1** does not represent the inherent ring-contraction regiospecificity of **1** to **18**. Although **19** is not formed from **1**, its yield rises as **18** is depleted by **18*** → **19**. Rapid trapping of **18** and **19** at T = −196 °C prevents their equilibration at T = 250 °C.

The alkyl group of 2-alkyl-substituted cyclobutylidenes **11** seldom undergoes a 1,2-C atom shift (Scheme 3c). Thus, a preference for ring-contraction **1** → **18** over ring-expansion **1** → **20** is understandable. The observed ring-contraction vs ring-expansion regioselectivity ratio of 6.7:1 is converse to the selectivity of **3**, which undergoes regiospecific ring-expansion to **6**. A rationale for the discordant behavior of carbenes **1** and **3** was developed with the aid of computational chemistry. Both **1** and **3** are predicted to have singlet ground states. The singlet−triplet energy gap (ΔE_{S-T}) between ^{1}**3** and ^{3}**3** is −9.0 kcal/mol, but that between ^{1}(+*ac*)-**1a** and ^{3}(+*ac*)-**1** is only −5.2 kcal/mol. The other difference between **1** and **3** is structural. The four-membered rings of **1** and **3** have unlike geometries. The 1°-ring of **1** is puckered whereas that of **3** is *flat*. Despite the high energy and high ring-strain energy of **6**, planarity of the cyclobutylidene moiety of **3** lowers the energy of ring-expansion TS(**3**/**6**) to the extent that other [1,2]-sigmatropic rearrangements are noncompetitive. An intramolecular orbital interaction between the highest occupied Walsh orbital of the three-membered 2°-ring and the unoccupied p orbital of the divalent C atom of the 1°-ring is responsible for this effect, which is not possible in **1** because it lacks Walsh orbitals (i.e., the 2°-ring of **1** is a four-membered ring). Homologization of **3** to **1** dramatically affects the positions of conformational energy minima. The optimal 1°-ring-puckering dihedral angle ($\phi_{1°}$) for **3** is 0°, but it is 19° for (+*ac*)-**1b** and 65° for (+*ac*)-**1a**. Carbene **1a** is predisposed to form **18** while **20** originates from **1b**, which has a flatter 1°-ring than **1a**. Thus, ring-expansion to **20** competes with ring-contraction to **18**, which is regiospecific because the energy barrier to **19** is too high.

The well-documented **9**:**8** ratio derived from **2** is (8.7 ± 4):1. The (**12a**−**12c**):(**12d**,**12e**) ratio derived from 2-alkyl-substituted cyclobutylidenes **11** is much greater. Thus, the predilection for **1** to undergo 1,2-C atom shift(s) in lieu of 1,2-H atom shift should be overriding because **1** is a 2,2-dialkyl-substituted cyclobutylidene. The chance that **22** is **22c** is therefore remote. Increased alkyl substitution on the C atom adjacent to the divalent C atom of **2** impedes 1,2-H atom shifts. This may be due to the degree of hyperconjugation within cyclobutylidenes, which increases as the four-membered ring ϕ value decreases.

EXPERIMENTAL SECTION

Computational Methods. Quantum chemical calculations were performed using the *Spartan'14 Parallel Suite* computer program.[78] Single-determinant (un)restricted Hartree−Fock ((U)HF) wave functions for molecules were corrected for electron−electron correlation using density functional theory (DFT) or quadratically convergent configuration interaction (QCI). The gas-phase molecules' equilibrium geometries were optimized using the (U)B3LYP/6-31G(d) theoretical model with the program's BigGrid option: exchange = 0.20 HF + 0.08 Slater +0.72 Becke[79] and correlation = 0.81 LYP[80] + 0.19 VWN1-RPA.[81] Normal mode vibrational analyses were performed at the level of geometry optimization. The harmonic vibrational frequencies were used to obtain temperature-independent zero-point vibrational energy (E_{ZPVE})[82] and temperature-dependent thermal vibrational energy (H_{vib}) values. Each TS had one and only one normal mode with an imaginary frequency ($\overline{\nu}_{TS}$). An intrinsic reaction coordinate (IRC) was generated to follow the transformation of reactant to product whenever possible. Single-point energy (E) values were computed using the higher-level UQCISD(T)(fc)/6-311G(d,p) theoretical model. Frozen-core (fc) multiple-determinant unrestricted wave functions were generated by single and (corrective) double excitations of valence electrons with (corrective) perturbative treatment of connected triple excitations. Before being added to E (T

DOI: 10.1021/acs.joc.6b02445
J. Org. Chem. 2016, 81, 12388−12400

= 0 K; p = 0 atm), all E_{ZPVE} values were scaled by the recommended Z factor of 0.9826.[83] Relative energy values ($\Delta_{rel}E$) and activation energy (E_a) values are specified relative to a reference molecule or to a reactant, respectively. Conversion of E values to enthalpy (H) values (computational STP: T = 298.15 K; p = 1 atm) was done according to eq S1 (see the Supporting Information). All H_{vib} (T = 298.15 K) values were scaled by the recommended H factor of 1.0004[83] before being added to the ZPVE-corrected E values. The increase in kinetic energy, due to translations (3(1/2)RT) and rotations (3(1/2)RT), for each nonlinear molecule was then added. Finally, RT (i.e., "pV work" needed to expand 1 mol of ideal gas to V = 24.465 L at T = 298.15 K and p = 1 atm) was added to obtain H (eq S1). Hess's Law was used to obtain $\Delta H°$ for each balanced homodesmotic bond-separation reaction (see the Table S2).

General Information. Melting points were measured on a melting point microscope and are uncorrected. The FT-NMR spectra were recorded at T = 300 K while the following radio frequencies were applied: $\nu(^1H)$ = 400.1 MHz and $\nu(^{13}C)$ = 100.6 MHz. Hydrogen-1 and carbon-13 chemical shift (δ) values are reported relative to tetramethylsilane (TMS), although the residual peaks of deuterated solvents were used to calibrate the ^1H and ^{13}C NMR spectra: $\delta_H(CDCl_3)$ = 7.26 ppm and $\delta_C(CDCl_3)$ = 77.16 ppm. Absolute values of coupling constants (|J|) are reported in hertz. MS analyses were conducted using an EI mass-selective detector (70 eV). Results are reported as m/z (% relative intensity). Analytical GC analyses were conducted using a 114.5 m poly(dimethylsiloxane) capillary (glass) column (silicone OV-101), a flame-ionization detector (T_{FID} = 250 °C), and a split-injector system (splitter-vent flow =1.5 mL He/min). Details of preparative GC are provided for specific products. Elemental analyses were performed using standard techniques.

1-(1-Ethoxycyclopropyl)cyclobutanol (14). **CAUTION!** A 1-L three-necked flask was outfitted with a mechanical stirrer and flushed with N_2 gas through the inlet and outlet openings. Inert-gas techniques using a flexible metal cannula were used to safely transfer 168 mL 1.7 M *t*-BuLi (**CAUTION!** pyrophoric on contact with atmospheric moisture) to the flask. All additions of organic liquids were carried out according to this safety method. The flask and its contents were cooled to T = −78 °C with stirring. Then 1-bromo-1-ethoxycyclopropane (**13**; 25.2 g, 153 mmol),[33−36] dissolved in 450 mL dry Et_2O, was cannulated into the reaction vessel. The solution was stirred for 20 min at T = −78 °C. A solution of cyclobutanone[84−86] (7 g, 100 mmol) in 80 mL dry Et_2O was precooled to T = −78 °C and then cannulated into this mixture. The contents of the flask were stirred at this temperature for an additional 20 min. The mixture was thawed to T = 0 °C and treated with about 250 mL saturated NH_4Cl. The aqueous phase was shaken twice with 200 mL Et_2O, and the combined organic extracts were dried over $MgSO_4$. The drying agent was filtered off, and the solvent was removed on a rotary evaporator. The residue was distilled at 0.06 Torr and a distillation head temperature of 42−45 °C. Alcohol **14** (15.15 g, 97.0 mmol, 97%) was 97% pure. It was further purified by preparative GC separation: (20% Carbowax + KOH, 1.6 m, T_{oven} = 140 °C, T_{TCD} = 160 °C, $T_{injector}$ = 160 °C, carrier flow = 145 mL He/min; 99.99% purity): δ_H/ppm (400.1 MHz, $CDCl_3$) 0.35−0.40 (2 H, m), 0.46−0.52 (2 H, m), 0.75−0.82 (3 H, t, ^3J 7), 1.16−1.37 (1 H, m), 1.51−1.64 (1 H, m), 1.65−1.78 (4 H, m), 3.11−3.19 (1 H, br s), 3.25−3.33 (2 H, "quart", ^3J 7); δ_C/ppm (100.6 MHz, $CDCl_3$) 8.6 (2 × CH_2), 12.8 (CH_2), 15.4 (CH_3), 33.2 (2 × CH_2), 63.8 (CH_2), 63.9 (C), 77.1 (C); $\bar{\nu}$ /cm^{-1} (film) 3440, 3100, 2980, 2940, 2880, 1450, 1415, 1390, 1250, 1150, 1110, 1065, 1010, 970, 910; m/z (EI, 70 eV) 156 (M^+, 0), 128 ([M − C_2H_4]$^+$, 56), 100 (95), 99 (63), 83 (12), 82 (20), 81 (10), 72 (11), 67 (16), 58 (25), 57 (68), 55 (26), 43 (100), 41 (30), 39 (24). Anal. Calcd for $C_9H_{16}O_2$: C, 69.19; H, 10.32. Found: C, 69.06; H, 10.29.

Spiro[3.3]heptan-1-one (15).[37] A mixture of alcohol **14** (15 g, 96 mmol) and 100 mL 50% HBF_4 in 1.3 L Et_2O was stirred magnetically for 3 days in a 2-L round-bottomed flask[36] and then neutralized with saturated Na_2CO_3 (**CAUTION!** violent reaction!). The organic phase was separated. The aqueous phase was extracted twice with 200 mL Et_2O. The combined organic phases were dried over $MgSO_4$, the drying agent was filtered off, and the solvent was removed over a 25-cm Vigreux column. The residue was distilled at 0.005 Torr with a boiling point of 30−32 °C. The yield of ketone **15** was 8.5 g (77 mmol, 80%). Further purification was conducted for spectroscopic purposes using preparative GC separation (20% DC-200, 1.6 m, T_{oven} = 150 °C, T_{TCD} = 170 °C, $T_{injector}$ = 170 °C, carrier flow = 120 mL He/min; 99.7% purity): δ_H/ppm (400.1 MHz, $CDCl_3$) 1.73−2.08 (6 H, m), 2.28−2.36 (2 H, m), 3.31−3.37 (2 H, t); δ_C/ppm (100.6 MHz, $CDCl_3$) 16.2 (CH_2), 24.9 (CH_2), 30.1 (2 × CH_2), 42.5 (CH_2), 63.9 (C), 214.1 (C); $\bar{\nu}$ /cm^{-1} (film) 2970, 2930, 2865, 2855, 1760, 1440, 1390, 1270, 1160, 1140, 1045; m/z (EI, 70 eV) 110 (M^+, 18), 82 (38), 68 (32), 67 (64), 57 (11), 54 (100), 53 (26), 43 (10), 41 (20), 40 (34), 39 (56).

Spiro[3.3]heptan-1-one p-Tosylhydrazone (16). *p*-Tosylhydrazide (9.18 g, 49.3 mmol) was dissolved in hot EtOH in a 100 mL flask. Ketone **15** (4.5 g, 41 mmol) was immediately added to the still-warm solution. *p*-Tosylhydrazone **16** precipitated over 2−3 h as fine needles. The white solid was filtered off and dried in vacuo. Recrystallization from EtOH afforded pure *p*-tosylhydrazone **16** (9.7 g, 35 mmol, 85%): mp 135 °C; δ_H/ppm (400.1 MHz, $CDCl_3$) 1.75−2.05 (6 H, m), 2.20−2.30 (2 H, m), 2.42−2.45 (3 H, s), 2.55−2.60 2 H, t, ^3J 8), 7.27−7.30 (1 H, br s), 7.30−7.38 (2 H, d, ^3J 8), 7.78−7.86 2 H, d, ^3J 8); δ_C/ppm (100.6 MHz, $CDCl_3$) 17.8 (CH_2), 23.2 (CH_3), 29.5 (2 × CH_2), 30.6 (CH_2), 34.5 (CH_2), 129.7 (2 × CH), 131.3 (2 × CH), 137.9 (C), 146.0 (C), 168.9 (C); $\bar{\nu}$ /cm^{-1} (film) 3200, 3020, 2980, 2940, 2860, 2810, 1910, 1665, 1590, 1490, 1410, 1400, 1330, 1280, 1230, 1210, 1180, 1150, 1120, 1090, 1070, 1010, 930, 900, 840, 810, 790, 750; m/z (EI, 70 eV) 278 (M^+, 8), 250 (2), 140 (10), 139 (33), 123 (100), 95 (24), 94 (28), 91 (45), 81 (10), 79 (55), 77 (28), 68 (12), 67 (45), 65 (37), 55 (32), 51 (10), 42 (24), 41 (50), 39 (42). Anal. Calcd for $C_{14}H_{18}N_2O_2S$: C, 60.41; H, 6.52; N, 10.06. Found: C, 60.51; H, 6.50; N, 10.18.

Spiro[3.3]heptan-1-one p-Tosylhydrazone Sodium Salt (17). **CAUTION!** A 50% NaH dispersion (1.88 g, 39 mmol) was added portionwise with stirring to a solution of *p*-tosylhydrazone **16** (9.5 g, 34 mmol) in 80 mL dry THF. Sodium salt **17** precipitated immediately with the evolution of H_2 gas. The mixture was stirred for 3 h, and then 350 mL dry pentane was added. Stirring was continued for another 3 h. The white solid was filtered off under inert gas due to its hygroscopicity. Sodium salt **17** was dried for 24 h in an oil pump vacuum to yield 10 g (33 mmol, 98%). It was stored in a vacuum desiccator.

High-Vacuum Flash Pyrolysis of 17. (See Figure S22 in the Supporting Information for a schematic of the HVFP apparatus.) Sodium salt **17** (0.35 g, 1.2 mmol) was transferred to a 250-mL, three-neck, round-bottomed flask under protective gas using a nonmetallic spatula. In order to maintain a high vacuum, **17** was released portionwise into the flask at T = 250 °C (metal bath) and p = ∼ 9 × 10^{-4} Torr (turbomolecular pump). A colorless pyrolysate was collected past the glass wool filter in the liquid N_2 trap. Residual solids (e.g., *p*-TsNa) were left behind. The vacuum pump valve was closed, the coldfinger was rotated 180°, and the coolant was allowed to dissipate. Then the volatile products were recondensed into a cooled receiving flask attached to the vacuum manifold. The condensate comprised five hydrocarbons (0.090 g, 82%). Four of them could be separated by preparative GC and spectroscopically characterized (see the Supporting Information), but a trace component could not be separated and identified. The products were formed in the following relative amounts: cyclopropylidenecyclobutane (**18**; 69.3%), 1-methylenespiro[2.3]hexane (**19**; 17.0%), bicyclo[3.2.0]hept-1(5)-ene (**20**; 8.6%), 1,2-dimethylenecyclopentane (**21**; 4.3%), and an unidentified hydrocarbon (**22**; 0.8%).

Cyclopropylidenecyclobutane (18): 20% DC-200, 4.5 m, T_{oven} = 100 °C, T_{TCD} = 120 °C, $T_{injector}$ = 125 °C, carrier flow = 120 mL He/min; 98.7% purity; δ_H/ppm (400.1 MHz, $CDCl_3$) 0.94−1.00 (4 H, quint, ^5J 2.5), 1.95−2.06 (2 H, quint, ^3J 8), 2.71−2.78 (4 H, tquint, ^3J 8, ^5J 2.5);[41,42] δ_C/ppm (100.6 MHz, $CDCl_3$) 1.8 (2 × CH_2), 17.4 (CH_2), 31.1 (2 × CH_2), 109.8 (C), 128.4 (C);[41] $\bar{\nu}$ /cm^{-1} (film) 3040, 2920, 2140, 2060, 2000, 1930, 1775, 1700, 1410, 1240, 1140, 1060, 1040, 965, 900, 870, 830, 760, 730, 705;[42,43] m/z (EI, 70 eV) 94 (M^+,

DOI: 10.1021/acs.joc.6b02445
J. Org. Chem. 2016, 81, 12388−12400

22), 93 (18), 91 (20), 79 (100), 77 (48), 66 (30), 65 (24), 51 (11), 40 (11), 39 (36).[41]

*1-Methylenespiro[2.3]hexane (**19**):* 20% DC-200, 4.5 m, T_{oven} = 100 °C, T_{TCD} = 120 °C, $T_{injector}$ = 125 °C, carrier flow = 120 mL He/min; 99.98% purity; δ_H/ppm (400.1 MHz, $CDCl_3$) 1.03−1.09 (2 H, t, ^4J 1.5), 1.92−2.12 (2 H, m), 2.12−2.23 (4 H, m), 5.35−5.39 (1 H, "s"), 5.40−5.45 (1 H, dt, ^2J 5, ^4J 1); 16.2 (CH_2), 16.8 (CH_2), 23.3 (C), 30.9 (2 × CH_2), 101.3 (CH_2), 140.7 (C); $\bar{\nu}$ /cm^{-1} (film) 3060, 3025, 2925, 2840, 1990, 1730, 1430, 1385, 1120, 1040, 1000, 940, 905, 875, 775, 730, 670;[44] *m*/*z* (EI, 70 eV) 94 (M^+, 2), 93 (17), 91 (12), 80 (8), 79 (100), 77 (37), 66 (21), 65 (20), 53 (14), 51 (11), 41 (10), 40 (24), 39 (46). Anal. Calcd for C_7H_{10}: C, 89.29; H, 10.70. Found: C, 89.18; H, 10.82.

*Bicyclo[3.2.0]hept-1(5)-ene (**20**):* 20% DC-200, 4.5 m, T_{oven} = 100 °C, T_{TCD} = 120 °C, $T_{injector}$ = 125 °C, carrier flow = 120 mL He/min; 99.4% purity; δ_H/ppm (400.1 MHz, $CDCl_3$) 1.98−2.06 (2 H, "quint", ^3J 7), 2.21−2.29 (4 H, "t", ^3J 7), 2.46−2.54 (4 H, t, ^3J 1.5);[45] δ_C/ppm (100.6 MHz, $CDCl_3$) 26.4 (CH_2), 27.9 (2 × CH_2), 31.4 (2 × CH_2), 149.6 (2 × C);[87] *m*/*z* (EI, 70 eV) 94 (M^+, 60), 93 (19), 91 (16), 79 (100), 77 (34), 39 (18).

*1,2-Dimethylenecyclopentane (**21**):*[48] 20% DC-200, 4.5 m, T_{oven} = 100 °C, T_{TCD} = 120 °C, $T_{injector}$ = 125 °C, carrier flow = 120 mL He/min; 100% purity; δ_H/ppm (400.1 MHz, $CDCl_3$) 1.60−1.70 (2 H, quint, ^3J 7), 2.40−2.54 (4 H, tt, ^3J 7, ^4J 1.5), 4.85−4.89 (2 H, t, ^4J 1.5), 5.31−5.35 (2 H, t, ^4J 1.5);[88] δ_C/ppm (100.6 MHz, $CDCl_3$) 24.1 (CH_2), 34.11 (2 × CH_2), 103.5 (2 × CH_2), 148.8 (2 × C);[89] *m*/*z* (EI, 70 eV) 95 ($[M + H]^+$, 5), 94 (M^+, 59), 93 (19), 91 (21), 79 (100), 77 (39), 39 (16).

*Spiro[3.3]heptan-1-ol (**24**).* Under inert gas, $LiAlH_4$ (0.73 g, 19.2 mmol) was suspended in 30 mL dry Et_2O in a 100 mL, two-necked flask outfitted with a reflux condenser and dropping funnel. Ketone **15** (1.5 g, 13.6 mmol), dissolved in 10 mL dry Et_2O, was added dropwise to the magnetically stirred suspension. The mixture was stirred overnight, and then excess $LiAlH_4$ was carefully destroyed with H_2O (**CAUTION!**). The organic phase was separated, and the aqueous phase was extracted with Et_2O (5 × 50 mL). The combined organic phases were dried over $MgSO_4$, the drying agent was filtered off, and the solvent was removed on a rotary evaporator. This gave alcohol **24** (1.20 g, 10.7 mmol, 78.6%) in 94.7% purity. A small amount was purified by preparative GC for spectroscopic purposes: 20% Carbowax + KOH, 1.6 m, T_{oven} = 140 °C, T_{TCD} = 160 °C, $T_{injector}$ = 145 °C, carrier flow = 145 mL He/min; 99.9% purity; δ_H/ppm (400.1 MHz, $CDCl_3$) 1.38−1.48 (1 H, dt, ^2J 7.5, ^3J 10); 1.49−1.60 (1 H, m); 1.66−1.77 (2 H, m), 1.77−1.99 (5 H, m), 2.07−2.16 (1 H, m), 2.28−2.37 (1 H, m), 3.81−3.88 (1 H, t, ^3J 7.5); δ_C/ppm (100.6 MHz, $CDCl_3$) 16.5 (CH_2), 26.4 (CH_2), 26.8 (CH_2), 28.2 (CH_2), 31.4 (CH_2), 49.6 (C), 72.3 (CH); $\bar{\nu}$ /cm^{-1} (film) 3310, 2965, 2930, 2860, 1430, 1325, 1270, 1255, 1210, 1160, 1130, 1080, 1020, 955, 915, 795; *m*/*z* (EI, 70 eV) 112 (M^+, 0.2), 111 (0.4), 97 (5.3), 84 (54), 83 (53), 79 (34), 69 (29), 68 (66), 67 (100), 57 (16), 56 (37), 55 (54), 53 (34), 44 (20), 43 (23), 42 (16), 41 (57), 40 (55), 39 (57). Anal. Calcd for $C_7H_{12}O$: C, 74.95; H, 10.78. Found: C, 74.84; H, 10.74.

*Spiro[3.3]hept-1-yl p-Tosylate (**25**).* Alcohol **24** (3 g, 26.7 mmol) and *p*-tosyl chloride (5.08 g, 26.7 mmol) were added under ice-cooling to a 50-mL round-bottomed flask that was filled with 25 mL of pyridine. The flask was refrigerated for 4 days at ∼5 °C. The contents were poured onto ice, and the aqueous phase was extracted with Et_2O (5 × 100 mL). The combined organic phases were dried over $MgSO_4$, the drying agent was filtered off, and the Et_2O was removed on a rotary evaporator. Residual pyridine was removed with an oil pump vacuum. This afforded 6.05 g (22.7 mmol, 85%) *p*-tosylate **25**. The *p*-tosylate was purified by HPLC for spectroscopic purposes: eluent Et_2O/*n*-C_5H_{12}, 1:4; δ_H/ppm (400.1 MHz, $CDCl_3$) 1.38−1.47 (1 H, m), 1.60−1.86 (7 H, m), 1.90−1.98 (1 H, m), 2.36−2.41 (3 H, s), 2.41−2.47 (1 H, m), 4.39−4.45 (1 H, t, ^3J 7), 7.26−7.34 (2 H, d, ^3J 8), 7.73−7.78 (2 H, d, ^3J 8); δ_C/ppm (100.6 MHz, $CDCl_3$) 16.1 (CH_2), 21.5 (CH_3), 25.8 (CH_2), 26.6 (CH_2), 28.2 (CH_2), 30.7 (CH_2), 48.7 (C), 78.9 (CH), 127.6 (2 × CH), 129.6 (2 × CH), 134.0 (C), 144.5 (C); $\bar{\nu}$ /cm^{-1} (film) 3080, 3060, 3030, 2970, 2930, 2860, 1600, 1495, 1450, 1435, 1400, 1365, 1310, 1290, 1210, 1190, 1180, 1120, 1100, 1035, 1005, 955, 945, 920, 880, 860, 815, 800, 795, 760, 705, 665; *m*/*z* (EI, 70 eV) 266 (M^+, 0), 238 (3.3), 225 (1.5), 199 (1.9), 198 (1.8), 155 (86), 111 (56), 95 (11), 94 (36), 93 (21), 92 (12), 91 (100), 83 (18), 81 (12), 79 (24), 68 (29), 67 (53), 65 (27), 55 (41), 53 (10), 41 (36), 39 (24). Anal. Calcd for $C_{14}H_{18}O_3S$: C, 63.13; H, 6.81. Found: C, 63.20; H, 6.91.

*Spiro[3.3]hept-1-ene (**22c**).* Potassium *tert*-butanolate (0.575 g, 5.13 mmol) was dissolved in dry DMSO (50 mL) in a 100-mL, two-necked, round-bottomed flask outfitted with a septum and condenser with a cold trap. The apparatus was evacuated to 0.02 Torr, and the cold trap was cooled with liquid N_2. A solution of **25** (1.00 g, 3.75 mmol) in 30 mL dry DMSO was introduced portionwise through the septum using a syringe. The resulting hydrocarbons were collected in the cold trap. The condensate was thawed at room temperature while the apparatus was vented with N_2 gas. Pentane (20 mL) was added, and the mixture was recondensed to get rid of entrained DMSO. After the solution was dried over $MgSO_4$, the drying agent was filtered off, and the solvent was distilled using a 25-cm Vigreux column. This gave spiro[3.3]hept-1-ene (0.247 g, 2.62 mmol, 70%) in a purity of 84.2%. The product was further purified via preparative GC: 20% DC-200, 4.5 m, T_{oven} = 100 °C, T_{TCD} = 120 °C, $T_{injector}$ = 125 °C, carrier flow = 120 mL He/min; 100% purity; δ_H/ppm (400.1 MHz, $CDCl_3$) 1.70−1.90 (2 H, m, ^2J 10.5, ^3J 8), 2.05−2.19 (4 H, m), 2.46−2.52 (2 H, "s"), 6.00−6.07 (1 H, "d", ^3J 2.5), 6.08−6.14 (1 H, d, ^3J 2.5);[51] δ_C/ppm (100.6 MHz, $CDCl_3$) 16.2 (CH_2), 31.8 (2 × CH_2), 44.8 (CH_2), 51.8 (C), 133.8 (CH), 142.9 (CH); $\bar{\nu}$ /cm^{-1} (film) 3230, 3155, 3080, 3060, 3040, 3020, 2980, 2960, 2940, 1670, 1615, 1550, 1485, 1360, 1310, 1250, 1220, 1180, 1080, 1010, 990, 970, 940, 910, 810, 760; *m*/*z* (EI, 70 eV) 93 ($[M - H]^+$, 2), 91 (3), 79 (19), 66 (100), 65 (14), 40 (16), 39 (24). Anal. Calcd for C_7H_{10}: C, 89.29; H, 10.70. Found: C, 89.22; H, 10.68.

*Triphenyl(prop-2-en-1-yl)phosphonium Bromide (**26**).* 3-Bromoprop-1-ene (120.98 g, 1.000 mol) and triphenylphosphine (150 g, 0.572 mol) were refluxed in 250 mL toluene overnight. The resulting white solid was filtered off, washed several times with toluene, and air-dried to give salt **26** (214 g, 0.558 mol, 98%).

*(Prop-2-en-1-ylidene)cyclobutane (**22d**).* Sodium amide (4.02 g, 100 mmol) was added to a stirred suspension of phosphonium bromide **26** (35.7 g, 93 mmol) in 200 mL dry Et_2O. The mixture was refluxed overnight and then cooled to give red-colored ylide **27**. Cyclobutanone[84−86] (5.0 g, 71 mmol) was added, the dark mixture was stirred 3 h, and then it was refluxed for 30 min. After the mixture was cooled, the solid was filtered off, and the filtrate was carefully distilled using a Vigreux column. The crude product (3 g, 32 mmol, 45%) was isolated with a purity of 86.7%. It was further purified via preparative GC to remove the remaining benzene and toluene: 20% DC-200, 4.5 m, T_{oven} = 70 °C, T_{TCD} = 90 °C, $T_{injector}$ = 90 °C, carrier flow = 120 mL He/min; 100% purity; δ_H/ppm (400.1 MHz, $CDCl_3$) 1.94−2.04 (2 H, quint, ^3J 8), 2.66−3.79 (4 H, "dt", ^2J 20, ^3J 8), 4.86−4.92 (1 H, doct, $^{long\text{-}range+2}J$ 1, ^3J 10), 4.95−5.02 (1 H, doct, $^{long\text{-}range,2}J$ 1, ^3J 17), 5.71−5.78 (1 H, "dt", ^3J 11), 6.18−6.30 (1 H, ddd, ^3J 10, ^3J 11, ^3J 17); δ_C/ppm (100.6 MHz, $CDCl_3$) 17.1 (CH_2), 29.9 (CH_2), 31.3 (CH_2), 113.0 (CH_2), 121.5 (CH), 133.1 (CH), 146.3 (C); $\bar{\nu}$ /cm^{-1} (film) 3080, 3040, 3010, 2980, 2950, 2910, 1670, 1600, 1420, 1190, 1015, 990, 890, 640; *m*/*z* (EI, 70 eV) 94 (M^+, 56), 93 (14), 91 (19), 79 (100), 77 (50), 66 (67), 65 (30), 54 (13), 53 (12), 51 (12), 41 (12), 40 (32), 39 (63). Anal. Calcd for C_7H_{10}: C, 89.29; H, 10.70. Found: C, 89.18; H, 10.71.

■ ASSOCIATED CONTENT

Supporting Information

The Supporting Information is available free of charge on the ACS Publications website at DOI: 10.1021/acs.joc.6b02445.

NMR spectra for compounds **14**−**16**, **18**−**21**, **22c**,**d**, **24**, and **25** as well as computational data for molecules in Chart 1, Tables 2−6, and Figures S23−S27 (PDF)

DOI: 10.1021/acs.joc.6b02445
J. Org. Chem. 2016, 81, 12388−12400

AUTHOR INFORMATION

Corresponding Author

*E-mail: udo.brinker@univie.ac.at, ubrinker@binghamton.edu.

ORCID

Murray G. Rosenberg: 0000-0001-8353-1736

Present Address

[§]Some material taken from the Ph.D. Dissertation of T.S., Ruhr-University Bochum, Bochum, Germany, 1989.

Notes

The authors declare no competing financial interest.

ACKNOWLEDGMENTS

Informative discussions with Professor Barry K. Carpenter, School of Chemistry, Cardiff University, Wales, regarding the computational aspects of this report are much appreciated.

REFERENCES

(1) Hine, J. *Divalent Carbon*; Ronald Press: New York, 1964.
(2) Kirmse, W. *Carbene Chemistry*, 2nd ed.; Academic: New York, 1971.
(3) (a) *Carbenes*; Jones, M., Jr., Moss, R. A., Eds.; Wiley: New York, 1973; Vol. *1*. (b) *Carbenes*; Moss, R. A., Jones, M., Jr., Eds.; Wiley: New York, 1975; Vol. *2*.
(4) *Methoden der Organischen Chemie (Houben-Weyl)*; Regitz, M., Ed.; Thieme: Stuttgart, 1989; Vol. *E19b*.
(5) (a) *Advances in Carbene Chemistry*; Brinker, U. H., Ed.; JAI: Greenwich, CT, 1994; Vol. *1*. (b) *Advances in Carbene Chemistry*; Brinker, U. H., Ed.; JAI: Stamford, CT, 1998; Vol. *2*. (c) *Advances in Carbene Chemistry*; Brinker, U. H., Ed.; Elsevier: Amsterdam, 2001; Vol. *3*.
(6) *Carbene Chemistry: From Fleeting Intermediates to Powerful Reagents*; Bertrand, G., Ed.; Dekker: New York, 2002.
(7) *Contemporary Carbene Chemistry*; Moss, R. A., Doyle, M. P., Eds.; Wiley: Hoboken, NJ, 2014.
(8) Jones, W. M.; Brinker, U. H. In *Pericyclic Reactions*; Marchand, A. P., Lehr, R. E., Eds.; Academic: New York, 1977; Vol. *1*, Chapter 3, pp 109−198.
(9) Bachrach, S. M. *Computational Organic Chemistry*, 2nd ed.; Wiley: Hoboken, NJ, 2014; p 297.
(10) Backes, J.; Brinker, U. H. Cyclobutylidene. In *Carbene(Carbenoide)*; Regitz, M., Ed.; Methoden der Organischen Chemie (Houben−Weyl); Thieme: Stuttgart, 1989; Vol. *E19b*, pp 511−541.
(11) Wiberg, K. B.; Burgmaier, G. J.; Warner, P. *J. Am. Chem. Soc.* **1971**, *93*, 246−247.
(12) Wiberg, K. B.; Matturro, M. G.; Okarma, P. J.; Jason, M. E.; Dailey, W. P.; Burgmaier, G. J.; Bailey, W. F.; Warner, P. *Tetrahedron* **1986**, *42*, 1895−1902.
(13) Wiberg, K. B.; Hiatt, J. E.; Burgmaier, G. J. *Tetrahedron Lett.* **1968**, *9*, 5855−5857.
(14) Brinker, U. H.; Boxberger, M. *Angew. Chem., Int. Ed. Engl.* **1984**, *23*, 974−975.
(15) Brinker, U. H.; Weber, J. *Tetrahedron Lett.* **1986**, *27*, 5371−5374.
(16) Brinker, U. H.; Schenker, G. *J. Chem. Soc., Chem. Commun.* **1982**, 679−681.
(17) Friedman, L.; Shechter, H. *J. Am. Chem. Soc.* **1960**, *82*, 1002−1003.
(18) Schoeller, W. W. *J. Am. Chem. Soc.* **1979**, *101*, 4811−4815.
(19) Sulzbach, H. M.; Platz, M. S.; Schaefer, H. F., III; Hadad, C. M. *J. Am. Chem. Soc.* **1997**, *119*, 5682−5689.
(20) Stracener, L. L.; Halter, R. J.; McMahon, R. J.; Castro, C.; Karney, W. L. *J. Org. Chem.* **2000**, *65*, 199−204.
(21) Pezacki, J. P.; Pole, D. L.; Warkentin, J.; Chen, T.; Ford, F.; Toscano, J. P.; Fell, J.; Platz, M. S. *J. Am. Chem. Soc.* **1997**, *119*, 3191−3192.
(22) Note that a spurious bond between C1 and C3 will be drawn in a graphical user interface if the bond-length cutoff is set too high.
(23) Carpenter, B. K. *Chem. Rev.* **2013**, *113*, 7265−7286.
(24) Bozkaya, U.; Özkan, İ. *J. Phys. Chem. A* **2012**, *116*, 2309−2321.
(25) Slipchenko, L. V.; Krylov, A. I. *J. Chem. Phys.* **2003**, *118*, 6874−6883.
(26) Davidson, E. R.; Borden, W. T. *J. Am. Chem. Soc.* **1977**, *99*, 2053−2060.
(27) Wiberg, K. B. *Angew. Chem., Int. Ed. Engl.* **1986**, *25*, 312−322.
(28) Bach, R. D.; Dmitrenko, O. *J. Am. Chem. Soc.* **2004**, *126*, 4444−4452.
(29) Dudev, T.; Lim, C. *J. Am. Chem. Soc.* **1998**, *120*, 4450−4458.
(30) Nordvik, T.; Mieusset, J.-L.; Brinker, U. H. *Org. Lett.* **2004**, *6*, 715−718.
(31) Brinker, U. H.; König, L. *J. Am. Chem. Soc.* **1979**, *101*, 4738−4739. Brinker, U. H.; König, L. *J. Am. Chem. Soc.* **1981**, *103*, 212−214.
(32) Brinker, U. H.; König, L. *Chem. Ber.* **1983**, *116*, 882−893. Brinker, U. H.; König, L. *Chem. Ber.* **1983**, *116*, 894−910.
(33) Salaün, J.; Marguerite, J. *Org. Synth.* **1985**, *63*, 147−153.
(34) Gadwood, R. C. *Tetrahedron Lett.* **1984**, *25*, 5851−5854.
(35) Gadwood, R. C.; Rubino, M. R.; Nagarajan, S. C.; Michel, S. T. *J. Org. Chem.* **1985**, *50*, 3255−3260.
(36) Miller, S. A.; Gadwood, R. C. *Org. Synth.* **1989**, *67*, 210−221.
(37) Trost, B. M.; Keeley, D. E.; Arndt, H. C.; Bogdanowicz, M. J. *J. Am. Chem. Soc.* **1977**, *99*, 3088−3100.
(38) Shapiro, R. H. *Org. React. (NY)* **1976**, *23*, 405−507.
(39) Dolbier, W. R., Jr.; Riemann, J. M.; Akiba, K.; Bertrand, M.; Bézaguet, A. *J. Chem. Soc. D* **1970**, 718−719.
(40) Dolbier, W. R., Jr.; Akiba, K.; Riemann, J. M.; Harmon, C. A.; Bertrand, M.; Bezaguet, A.; Santelli, M. *J. Am. Chem. Soc.* **1971**, *93*, 3933−3940.
(41) Maercker, A.; Daub, V. E. E. *Tetrahedron* **1994**, *50*, 2439−2458.
(42) van den Heuvel, C. J. M.; Holland, A.; van Velzen, J. C.; Steinberg, H.; de Boer, Th. J. *Recl. Trav. Chim. Pays-Bas* **1984**, *103*, 233−240.
(43) Vincent, J.-P.; Bezaguet, A.; Bertrand, M. *Bull. Soc. Chim. Fr.* **1967**, 3550−3551.
(44) Bertrand, M. *Bull. Soc. Chim. Fr.* **1968**, 3044−3054.
(45) Kirmse, W.; Pook, K. H. *Angew. Chem., Int. Ed. Engl.* **1966**, *5*, 594.
(46) Bachrach, S. M.; Gilbert, J. C. *J. Org. Chem.* **2004**, *69*, 6357−6364.
(47) Glowacki, D. R.; Marsden, S. P.; Pilling, M. J. *J. Am. Chem. Soc.* **2009**, *131*, 13896−13897.
(48) Blomquist, A. T.; Wolinsky, J.; Meinwald, Y. C.; Longone, D. T. *J. Am. Chem. Soc.* **1956**, *78*, 6057−6063.
(49) Lee, P. S.; Sakai, S.; Hörstermann, P.; Roth, W. R.; Kallel, E. A.; Houk, K. N. *J. Am. Chem. Soc.* **2003**, *125*, 5839−5848.
(50) Takeuchi, K.; Horiguchi, A.; Inagaki, S. *Tetrahedron* **2005**, *61*, 2601−2606.
(51) Roberts, C.; Walton, J. C.; Maillard, B. *J. Chem. Soc., Perkin Trans. 2* **1986**, 305−311.
(52) Le Perchec, P.; Conia, J. M. *Tetrahedron Lett.* **1970**, *11*, 1587−1588.
(53) Carpenter, B. K. Interpretation of Activation Parameters. *Determination of Organic Reaction Mechanisms*; Wiley-Interscience: New York, 1984; Chapter 7, pp 123−158.
(54) Carpenter, B. K. Cardiff University, Cardiff, U.K. Personal communication, 2016.
(55) Flowers, M. C.; Frey, H. M. *J. Am. Chem. Soc.* **1972**, *94*, 8636−8637.
(56) Wentrup, C. *Reactive Molecules: The Neutral Reactive Intermediates in Organic Chemistry*; Wiley: New York, 1984; pp 225−230.
(57) Wentrup, C. *Tetrahedron* **1974**, *30*, 1301−1311.
(58) Wang, X.; Agarwal, J.; Schaefer, H. F., III. *Phys. Chem. Chem. Phys.* **2016**, *18*, 24560−24568.
(59) Brinker, U. H.; Erdle, W. *Angew. Chem., Int. Ed. Engl.* **1987**, *26*, 1260−1262.

DOI: 10.1021/acs.joc.6b02445
J. Org. Chem. 2016, 81, 12388−12400

(60) Wiberg, K. B.; Fenoglio, R. A. *J. Am. Chem. Soc.* **1968**, *90*, 3395−3397.
(61) Greenberg, A.; Liebman, J. F. *Strained Organic Molecules*; Academic: New York, 1978; pp 298−299.
(62) Lafferty, W. J. Determination of Potential Functions and Barriers to Planarity for the Ring-Puckering Vibrations of Four-Membered Ring Molecules. In *Critical Evaluation of Chemical and Physical Structural Information*, Conference Proceedings, Dartmouth College, Jun 24−29, 1973; Lide, D. R., Jr., Paul, M. A., Eds.; National Academy of Sciences: Washington, DC, 1974; pp 386−409.
(63) Wiberg, K. B. *J. Org. Chem.* **1985**, *50*, 5285−5291.
(64) (a) Laane, J. *J. Phys. Chem.* **1991**, *95*, 9246−9249. (b) Laane, J. *Annu. Rev. Phys. Chem.* **1994**, *45*, 179−211.
(65) In lieu of such software, the value of ϕ_n also can be calculated directly from the 3-D Cartesian coordinates of the nonplanar four-membered ring. See the Supporting Information for an example based on **2**.
(66) Brinker, U. H.; Lin, G.; Xu, L.; Smith, W. B.; Mieusset, J.-L. *J. Org. Chem.* **2007**, *72*, 8434−8451.
(67) Herges, R. *Angew. Chem., Int. Ed. Engl.* **1994**, *33*, 255−276.
(68) Johnson, R. P.; Daoust, K. J. *J. Am. Chem. Soc.* **1995**, *117*, 362−367.
(69) Jensen, P.; Bunker, P. R. *J. Chem. Phys.* **1988**, *89*, 1327−1332.
(70) Gaspar, P. P.; Hammond, G. S. In *Carbenes*; Moss, R. A., Jones, M., Jr., Eds.; Wiley: New York, 1975; Vol. 2, Chapter 6, pp 207−362.
(71) Bachrach, S. M. *J. Chem. Educ.* **1990**, *67*, 907−908.
(72) George, P.; Trachtman, M.; Bock, C. W.; Brett, A. M. *Tetrahedron* **1976**, *32*, 317−323.
(73) George, P.; Trachtman, M.; Brett, A. M.; Bock, C. W. *J. Chem. Soc., Perkin Trans. 2* **1977**, 1036−1047.
(74) George, P.; Trachtman, M.; Bock, C. W.; Brett, A. M. *J. Chem. Soc., Perkin Trans. 2* **1976**, 1222−1227.
(75) Wheeler, S. E.; Houk, K. N.; Schleyer, P. v. R.; Allen, W. D. *J. Am. Chem. Soc.* **2009**, *131*, 2547−2560.
(76) Richey, H. G., Jr. In *Carbonium Ions: Major Types (Continued)*; Olah, G. A., Schleyer, P. v. R., Eds.; Reactive Intermediates in Organic Chemistry; Olah, G. A., Ed.; Wiley-Interscience: New York, 1972; Vol. 3, Chapter 25, pp 1201−1294.
(77) Wiberg, K. B.; Hess, B. A., Jr.; Ashe, A. J., III In *Carbonium Ions: Major Types (Continued)*; Olah, G. A.; Schleyer, P. v. R., Eds.; Reactive Intermediates in Organic Chemistry, Olah, G. A., Ed.; Wiley-Interscience: New York, 1972; Vol. 3, Chapter 26, pp 1295−1345.
(78) *Spartan'14 Parallel Suite*, version 1.1.8; Wavefunction Inc.: Irvine, CA, 2013.
(79) Becke, A. D. *J. Chem. Phys.* **1993**, *98*, 5648−5652.
(80) Lee, C.; Yang, W.; Parr, R. G. *Phys. Rev. B: Condens. Matter Mater. Phys.* **1988**, *37*, 785−789.
(81) Hehre, W. J. *A Guide to Molecular Mechanics and Quantum Chemical Calculations*; Wavefunction, Inc.: Irvine, CA, 2003.
(82) Csonka, G. I.; Ruzsinszky, A.; Perdew, J. P. *J. Phys. Chem. A* **2005**, *109*, 6779−6789.
(83) (a) Frequency Scale Factors for E_{ZPVE} and $H_{vib}(T)$. Radom Group Scale Factors. http://groups.chem.usyd.edu.au/radom/More/ScaleFactor.html (accessed Oct. 5, 2016). (b) Merrick, J. P.; Moran, D.; Radom, L. *J. Phys. Chem. A* **2007**, *111*, 11683−11700. (c) Scott, A. P.; Radom, L. *J. Phys. Chem.* **1996**, *100*, 16502−16513.
(84) Krumpolc, M.; Rocek, J. *Org. Synth.* **1981**, *60*, 20−25.
(85) Weber, J.; Haslinger, U.; Brinker, U. H. *J. Org. Chem.* **1999**, *64*, 6085−6086.
(86) Roberts, J. D.; Sauer, C. W. *J. Am. Chem. Soc.* **1949**, *71*, 3925−3929.
(87) Rasul, G.; Olah, G. A.; Surya Prakash, G. K. *J. Phys. Chem. A* **2006**, *110*, 7197−7201.
(88) van Straten, J. W.; van Norden, J. J.; van Schaik, T. A. M.; Franke, G. T.; De Wolf, W. H.; Bickelhaupt, F. *Recl. Trav. Chim. Pays-Bas* **1978**, *97*, 105−106.
(89) Stöcker, M.; Klessinger, M.; Wilhelm, K. *Org. Magn. Reson.* **1981**, *17*, 153−155.

DOI: 10.1021/acs.joc.6b02445
J. Org. Chem. 2016, 81, 12388−12400